AGOL CYCLES OF PSEUDO-ANOSOV MAPS ON THE 2-PUNCTURED TORUS AND 5-PUNCTURED SPHERE

JEAN-BAPTISTE BELLYNCK AND EIKO KIN

Abstract. Given a periodic splitting sequence of a measured train track, an Agol cycle is the part that constitutes a period up to the action of a pseudo-Anosov map and the rescaling by its dilatation. We consider a family of pseudo-Anosov maps on the 2-punctured torus and on the 5-punctured sphere. We present measured train tracks and compute their Agol cycles. We give a condition under which two maps in the defined family are conjugate or not. In the process, we find a new formula for the dilatation.

1. Introduction

Let $\Sigma = \Sigma_{g,n}$ be an orientable surface with genus g and n punctures. Let $\mathrm{MCG}(\Sigma)$ be the mapping class group of Σ. According to the Nielsen-Thurston-classification, every element of $\mathrm{MCG}(\Sigma)$ falls into 3 types: periodic, reducible and pseudo-Anosov. If $\phi\colon \Sigma \to \Sigma$ is a pseudo-Anosov map, then there exist associated stable and unstable measured laminations $(\mathcal{L}^s, \nu^s)$ and $(\mathcal{L}^u, \nu^u)$ and the dilatation $\lambda = \lambda(\phi) > 1$ such that

$$\phi(\mathcal{L}^s, \nu^s) = (\mathcal{L}^s, \lambda\nu^s) \text{ and } \phi(\mathcal{L}^u, \nu^u) = (\mathcal{L}^u, \lambda^{-1}\nu^u).$$

A *measured train track* (τ, μ) is a train track τ with a transverse measure μ. Edges of a train track are called *branches* and vertices are called *switches*. A branch that locally looks like the central branch in Figure 1(1) is called a *large branch*. A *splitting* at a large branch is an operation that gives a new measured train track. There are two kinds of splitting, *left* and *right splitting* at a large branch (Figure 1(2)(3)). See Definition 2.1.

A *maximal splitting* $(\tau_0, \mu_0) \rightharpoonup (\tau_1, \mu_1)$ is an operation on the measured train track (τ_0, μ_0) that splits all the large branches that carry maximal μ_0-weight and (τ_1, μ_1) is the resulting measured train track. If all the splittings in a maximal splitting are left (resp. right) splittings, the maximal splitting is denoted by $\overset{\mathrm{l}}{\rightharpoonup}$ (resp. $\overset{\mathrm{r}}{\rightharpoonup}$) and called a *left (resp. right) maximal splitting*.

It was proven by Agol that after enough maximal splittings the measured train track (τ, μ) suited to the stable measured lamination of a pseudo-Anosov map ϕ will have changed to $\phi(\tau, \lambda^{-1}\mu) := (\phi(\tau), \lambda^{-1}\phi_*(\mu))$, where the measure $\phi_*(\mu)$ is defined by $\phi_*(\mu)(e) :=$

Date: September 22, 2024.
Key words and phrases. pseudo-Anosov, periodic splitting sequences, Agol cycle length.

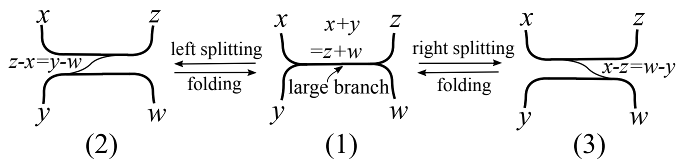

FIGURE 1. (1) A large branch. (2) Left splitting when $z > x$ ($\Leftrightarrow y > w$), (3) right splitting when $x > z$ ($\Leftrightarrow w > y$) at the large branch.

$\mu(\phi^{-1}(e))$ for a branch e in the train track $\phi(\tau)$. To state Agol's result precisely, a sequence of consecutive n maximal splittings $(\tau_0, \mu_0) \rightharpoonup \cdots \rightharpoonup (\tau_n, \mu_n)$ is denoted by $(\tau_0, \mu_0) \rightharpoonup^n (\tau_n, \mu_n)$.

Theorem 1.1 (Agol [1]. See also Agol-Tsang [2])**.** *Let $\phi\colon \Sigma \to \Sigma$ be a pseudo-Anosov map with dilatation λ. Let (τ, μ) be a measured train track suited to the stable measured lamination of ϕ. Then there exist $n \geq 0$ and $m > 0$ such that*

$$(\tau, \mu) \rightharpoonup^n (\tau_n, \mu_n) \rightharpoonup^m (\tau_{n+m}, \mu_{n+m}) = \phi(\tau_n, \lambda^{-1}\mu_n).$$

For the terminology *suited to*, see Definition 2.2. We call the maximal splitting sequence

$$(\tau_n, \mu_n) \rightharpoonup^m (\tau_{n+m}, \mu_{n+m}) \rightharpoonup^m (\tau_{n+2m}, \mu_{n+2m}) \rightharpoonup^m \cdots$$

a *periodic splitting sequence* of ϕ. We call the finite subsequence $(\tau_n, \mu_n) \rightharpoonup^m (\tau_{n+m}, \mu_{n+m})$ an *Agol cycle* of ϕ and call m the *Agol cycle length* of ϕ, denoted by $\ell(\phi)$. The *total splitting number* of an Agol cycle of ϕ, denoted by $N(\phi)$, is the number of large branches that are split in the Agol cycle (Definition 2.3(3)).

An *equivalence class* of an Agol cycle is a conjugacy invariant of pseudo-Anosov maps (Section 2.1). The Agol cycle length $\ell(\phi)$ and total splitting number $N(\phi)$ are conjugacy invariants as well. If $\phi : \Sigma \to \Sigma$ is fully-punctured (i.e., the singularities of the stable/unstable foliations of ϕ lie on the punctures of Σ), $N(\phi)$ equals the number of ideal tetrahedra in the veering triangulation of the mapping torus of ϕ. See [1] for more details.

It is natural to ask how the Agol cycle length $\ell(\phi)$ and total splitting number $N(\phi)$ relate to other invariants of pseudo-Anosov maps. In [6] it was proven that for every pseudo-Anosov 3-braid β, its Agol cycle length, the Garside canonical length of any element in the super summit set of β are the same. Agol-Tsang [2] proved that the total splitting number $N(\phi)$ for a fully punctured pseudo-Anosov $\phi : \Sigma \to \Sigma$ is bounded from above by a constant depending on the normalized dilatation $\lambda^{-\chi(\Sigma)}$, where $\chi(\Sigma)$ is the Euler characteristic of Σ.

The main goal of this paper is to give an explicit description of an Agol cycle of every pseudo-Anosov map in the two semigroups $F_T \subset \mathrm{MCG}(\Sigma_{1,2})$ and $F_D \subset \mathrm{MCG}(\Sigma_{0,5})$ which will be defined below. On the 2-punctured torus $\Sigma_{1,2}$, let δ_i be the right-handed Dehn twist about the simple closed curve $c_i \subset \Sigma_{1,2}$ for $i \in \{1, 2, 3\}$ shown in Figure 2(1). The hyperelliptic involution exchanges the two punctures of the torus and induces a 2-fold branched cover $\Sigma_{1,2} \to \Sigma_{0,5}$ of the 5-punctured sphere. Then δ_i descends to σ_i, the positive half-twist about the segment α_i connecting the punctures i and $i+1$ (Figure 2(5)).

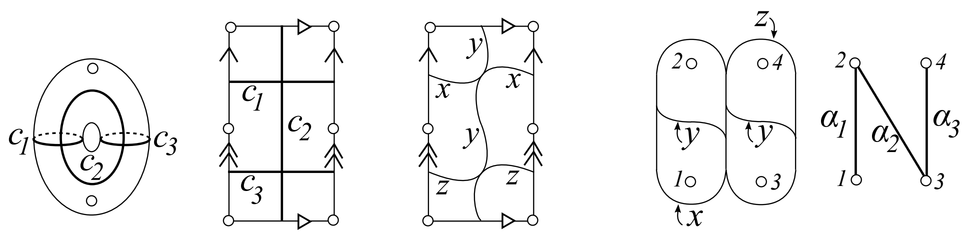

(1) (2) (3) (4) (5)

Figure 2. (1)(2) Simple closed curves c_1, c_2 and c_3 in $\Sigma_{1,2}$. (3) $(\mathfrak{b}, \boldsymbol{x})$ in $\Sigma_{1,2}$ and (4) $(\mathfrak{b}_L, \boldsymbol{x})$ in $\Sigma_{0,5}$ for $\boldsymbol{x} = \left(\begin{smallmatrix} x \\ y \\ z \end{smallmatrix}\right)$. (5) Segments α_i in $\Sigma_{0,5}$.

We study pseudo-Anosov maps in the semigroups

$$F_T := F(\delta_1, \delta_3, \delta_2^{-1}) \subset \mathrm{MCG}(\Sigma_{1,2}) \text{ and } F_D := F(\sigma_1, \sigma_3, \sigma_2^{-1}) \subset \mathrm{MCG}(\Sigma_{0,5})$$

generated by δ_1, δ_3 and δ_2^{-1} and by σ_1, σ_3 and σ_2^{-1}. Each σ_i for $i \in \{1,2,3\}$ fixes the fifth puncture of $\Sigma_{0,5}$. Hence, one can regard an element of F_D as a mapping class on the 4-punctured disk. The subset $\mathcal{I}_n \subset \mathbb{N}_0^{3n}$, where $\mathbb{N}_0 = \mathbb{N} \cup \{0\}$, will be useful for our study of pseudo-Anosov maps in F_T and F_D (Definition 2.9). For each $\boldsymbol{p} = (p_n, p'_n, q_n, ..., p_1, p'_1, q_1) \in \mathcal{I}_n$

$$\Phi_{\boldsymbol{p}} := \delta_1^{p_n} \delta_3^{p'_n} \delta_2^{-q_n} \cdots \delta_1^{p_1} \delta_3^{p'_1} \delta_2^{-q_1} \in F_T \text{ and } \phi_{\boldsymbol{p}} := \sigma_1^{p_n} \sigma_3^{p'_n} \sigma_2^{-q_n} \cdots \sigma_1^{p_1} \sigma_3^{p'_1} \sigma_2^{-q_1} \in F_D$$

are pseudo-Anosov maps. We take matrices $M_1 = \left(\begin{smallmatrix} 1&1&0 \\ 0&1&0 \\ 0&0&1 \end{smallmatrix}\right)$, $M_3 = \left(\begin{smallmatrix} 1&0&0 \\ 0&1&0 \\ 0&1&1 \end{smallmatrix}\right)$, $M_2 = \left(\begin{smallmatrix} 1&0&0 \\ 1&1&1 \\ 0&0&1 \end{smallmatrix}\right)$. For each $\boldsymbol{p} \in \mathcal{I}_n$ the matrix

$$M_{\boldsymbol{p}} := M_1^{p_n} M_3^{p'_n} M_2^{q_n} \cdots M_1^{p_1} M_3^{p'_1} M_2^{q_1}$$

is Perron-Frobenius. The Perron-Frobenius eigenvalue $\lambda_{\boldsymbol{p}}$ is equal to the dilatations of maps $\Phi_{\boldsymbol{p}}$ and $\phi_{\boldsymbol{p}}$. In Theorem 2.13 we present an explicit description of the Perron-Frobenius eigenvalue $\lambda_{\boldsymbol{p}}$ and the normalized eigenvector $\boldsymbol{v}_{\boldsymbol{p}}$. As a consequence we see that $\lambda_{\boldsymbol{p}}$ is a quadratic irrational (Remark 2.15). Let $\mathfrak{b} \subset \Sigma_{1,2}$ (resp. $(\mathfrak{b}_L \in \Sigma_{0,5})$ be train track as in Figure 2(3) (resp. Figure 2(4)). Assigning the coefficients of a Perron-Frobenius eigenvector $\boldsymbol{x}$ of $M_{\boldsymbol{p}}$ to the branches of the train track makes the measured train track $(\mathfrak{b}, \boldsymbol{x})$ (resp. $(\mathfrak{b}_L, \boldsymbol{x})$).

We say that $\boldsymbol{p} \in \mathcal{I}_n$ is *symmetric* if $p_i = p'_i$ for all $i \in \{1, \ldots, n\}$. Otherwise, $\boldsymbol{p}$ is *asymmetric*. To state our results, we use the symbol $\overset{\mathrm{l}}{\rightharpoonup}{}^{n}$ (resp. $\overset{\mathrm{r}}{\rightharpoonup}{}^{n}$) for n consecutive left (resp. right) maximal splittings.

Theorem 1.2. *For $\boldsymbol{p} = (p_n, p'_n, q_n, \ldots, p_1, p'_1, q_1) \in \mathcal{I}_n$ let $\Phi_{\boldsymbol{p}} \in F_T$ be the pseudo-Anosov map and $M_{\boldsymbol{p}}$ be the Perron-Frobenius matrix associated with $\boldsymbol{p}$. Let $\boldsymbol{v} > \boldsymbol{0}$ be an eigenvector* *with respect to the Perron-Frobenius eigenvalue $\lambda_{\boldsymbol{p}}$ of $M_{\boldsymbol{p}}$. Then the Agol cycle length ℓ of $\Phi_{\boldsymbol{p}}$ is*

$$\ell = \begin{cases} \sum_{i=1}^{n}(p_i + 2q_i) & \text{if } \boldsymbol{p} \text{ is symmetric,} \\ \sum_{i=1}^{n}(p_i + p_i' + 3q_i) & \text{if } \boldsymbol{p} \text{ is asymmetric.} \end{cases}$$

Moreover, starting with the measured train track $(\tau_0, \mu_0) = (\mathfrak{b}, \lambda_{\boldsymbol{p}}\boldsymbol{v})$, a finite subsequence of the maximal splitting sequence

$$(\tau_0, \mu_0) \overset{\mathrm{r}}{\rightharpoondown}^{p_n} \overset{\mathrm{l}}{\rightharpoondown}^{2q_n} \cdots \overset{\mathrm{r}}{\rightharpoondown}^{p_1} \overset{\mathrm{l}}{\rightharpoondown}^{2q_1} (\tau_\ell, \mu_\ell) \qquad \text{if } \boldsymbol{p} \text{ is symmetric,}$$

$$(\tau_0, \mu_0) \overset{\mathrm{r}}{\rightharpoondown}^{p_n + p_n'} \overset{\mathrm{l}}{\rightharpoondown}^{3q_n} \cdots \overset{\mathrm{r}}{\rightharpoondown}^{p_1 + p_1'} \overset{\mathrm{l}}{\rightharpoondown}^{3q_1} (\tau_\ell, \mu_\ell) \quad \text{if } \boldsymbol{p} \text{ is asymmetric}$$

forms an Agol cycle of $\Phi_{\boldsymbol{p}}$.

We later prove an analogous statement for the pseudo-Anosov maps $\phi_{\boldsymbol{p}} \in F_D$ inside the semi-group F_D (See Theorem 4.1).

As applications, we give formulas on the total splitting numbers $N(\Phi_{\boldsymbol{p}})$ and $N(\phi_{\boldsymbol{p}})$ for each $\boldsymbol{p} \in \mathcal{I}_n$ (Theorems 3.4, 4.8). We also classify conjugacy classes of pseudo-Anosov maps in F_T and F_D (Theorem 5.1). The total splitting numbers $N(\Phi_{\boldsymbol{p}})$ and $N(\phi_{\boldsymbol{p}})$ have the following additive property.

Theorem 1.3. *For $\boldsymbol{p} = (p_n, p_n', q_n, \dots, p_1, p_1', q_1) \in \mathcal{I}_n$ and $\boldsymbol{t} = (t_m, t_m', u_m, \dots, t_1, t_1', u_1) \in \mathcal{I}_m$, we set $\boldsymbol{pt} := (p_n, p_n', q_n, \dots, p_1, p_1', q_1, t_m, t_m', u_m, \dots, t_1, t_1', u_1) \in \mathcal{I}_{n+m}$. The total splitting number of $\Phi_{\boldsymbol{pt}} \in F_T$ satisfies $N(\Phi_{\boldsymbol{pt}}) = N(\Phi_{\boldsymbol{p}}) + N(\Phi_{\boldsymbol{t}})$. A parallel statement holds for $\phi_{\boldsymbol{pt}} \in F_D$.*

The paper is organized as follows. In Section 2 we recall basic definitions and prove lemmas. In Sections 3 and 4 we compute Agol cycles of pseudo-Anosov maps in F_T and F_D. In Section 5 we classify pseudo-Anosov conjugacy classes in F_T and F_D.

2. Preliminaries

The mapping class group $\mathrm{MCG}(\Sigma)$ of a surface $\Sigma = \Sigma_{g,n}$ is the group of isotopy classes of orientation preserving homeomorphisms of Σ preserving the punctures setwise. We apply elements of the mapping class group from right to left; i.e., the product fg means that we apply g, then f. For simplicity we do not distinguish between a homeomorphism $\phi : \Sigma \to \Sigma$ and its mapping class $[\phi] \in \mathrm{MCG}(\Sigma)$.

2.1. **Measured train tracks.**

A *train track* $\tau \subset \Sigma$ is a finite C^1-embedded graph, equipped with a well-defined tangent line at each vertex, also satisfying some additional properties as stated in Penner-Harer [8]. In this paper we assume our train tracks to be trivalent. A *measured train track* (τ, μ) is a train track τ with a measure μ. This is a function that assigns a positive weight to each branch. Measured train tracks are required to satisfy the *switch condition.* This means that if two branches a, b merge into one branch c, then the weights satisfy $\mu(a) + \mu(b) = \mu(c)$. See Figure 3(1).

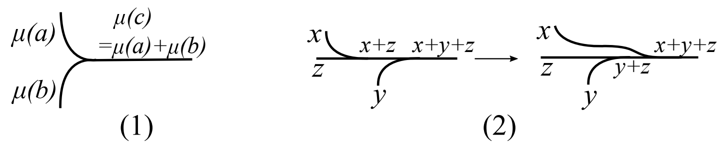

Figure 3. (1) Switch condition. (2) Shifting.

Definition 2.1. We consider a large branch as in Figure 1(1). Depending on weights x, y, z and w in Figure 1(1), a *splitting* divides a large branch into two branches and connects the two parts with either a left-facing or right-facing branch, thereby preserving the switch condition. Depending on the type of a branch inserted, the splitting is called a *left* or *right splitting* at a large branch (Figure 1(2)(3)). Similarly, we can produce new measured train tracks through the use of *folding* (Figure 1) and *shifting* (Figure 3(2)).

Recall that if all the splittings in a maximal splitting $(\tau_0, \mu_0) \rightharpoonup (\tau_1, \mu_1)$ are left (resp. right) splittings, the maximal splitting is denoted by $\overset{\mathrm{l}}{\rightharpoonup}$ (resp. $\overset{\mathrm{r}}{\rightharpoonup}$) and called a left (resp. right) maximal splitting. If there exist both left and right splittings, the maximal splitting is denoted by $\overset{\mathrm{lr}}{\rightharpoonup}$ and called a *mixed maximal splitting*.

Measured train tracks (τ, μ), (τ', μ') in Σ are *equal* (and write $(\tau, \mu) = (\tau', \mu')$) if there exists a diffeomorphism $f : \Sigma \to \Sigma$ isotopic to the identity map such that $f(\tau, \mu) = (\tau', \mu')$.

Measured train tracks (τ, μ), (τ', μ') in Σ are *equivalent* if they are related to each other by a sequence of splittings, foldings, shiftings and isotopies. Thus measured train tracks in a splitting sequence are equivalent. Equivalence classes of measured train tracks are in one-to-one correspondence with measured laminations [8, Theorem 2.8.5].

Definition 2.2. Let $(\mathcal{L}, \nu)$ be a measured lamination in Σ, and let (τ, μ) be a measured train track in Σ. Then (τ, μ) is *suited* to $(\mathcal{L}, \nu)$ if there exists a differentiable map $f : \Sigma \to \Sigma$ homotopic to the identity map on Σ with the following conditions:

- $f(\mathcal{L}) = \tau$.
- f is nonsingular on the tangent spaces to the leaves of $\mathcal{L}$.
- If p is an interior point of a branch e of τ then $\nu(f^{-1}(p)) = \mu(e)$.

Definition 2.3.

(1) The *splitting number of a maximal splitting* $(\tau_0, \mu_0) \rightharpoonup (\tau_1, \mu_1)$ is the number of large branches split, i.e., the number of the large branches of (τ_0, μ_0) with maximal weight.
(2) The *total splitting number of a finite sequence of maximal splittings* $(\tau, \mu) \rightharpoonup^n (\tau_n, \mu_n)$ is the sum of the splitting numbers over all maximal splittings in the finite sequence.
(3) The *total splitting number of an Agol cycle* $(\tau_n, \mu_n) \rightharpoonup^m (\tau_{n+m}, \mu_{n+m})$ of ϕ, denoted by $N(\phi)$, is the sum of the splitting numbers over all maximal splittings $(\tau_{n+i}, \mu_{n+i}) \rightharpoonup (\tau_{n+i+1}, \mu_{n+i+1})$ in the Agol cycle. The Agol cycle length $\ell(\phi)$ is less

than or equal to $N(\phi)$. The equality holds if and only if the splitting number of each maximal splitting in the Agol cycle is exactly 1.

Definition 2.4. Let $\phi, \phi' \colon \Sigma \to \Sigma$ be pseudo-Anosov maps with periodic splitting sequences

$$\mathscr{P} : (\tau_n, \mu_n) \rightharpoonup^m (\tau_{n+m}, \mu_{n+m}) = \phi(\tau_n, \lambda^{-1}\mu_n) \rightharpoonup \cdots$$

of ϕ and

$$\mathscr{P}' : (\tau'_{n'}, \mu'_{n'}) \rightharpoonup^{m'} (\tau'_{n'+m'}, \mu'_{n'+m'}) = \phi'(\tau'_{n'}, (\lambda')^{-1}\mu'_{n'}) \rightharpoonup \cdots$$

of ϕ'. We say that $\mathscr{P}$ and $\mathscr{P}'$ are *combinatorially isomorphic* ([5]) if $m = m'$ is fulfilled and there exist an orientation-preserving diffeomorphism $h \colon \Sigma \to \Sigma$, integers $p, q \in \mathbb{Z}_{\geq 0}$ and $c \in \mathbb{R}_{>0}$ such that the following conditions (1) and (2) hold.

(1) $\phi' = h \circ \phi \circ h^{-1}$.
(2) $h(\tau_{i+p}, \mu_{i+p}) = (\tau'_{i+q}, c\mu'_{i+q})$ for all $i \in \mathbb{Z}_{\geq 0}$.

We say that two Agol cycles $(\tau_n, \mu_n) \rightharpoonup^m (\tau_{n+m}, \mu_{n+m})$ of ϕ and $(\tau'_{n'}, \mu'_{n'}) \rightharpoonup^{m'} (\tau'_{n'+m'}, \mu'_{n'+m'})$ of ϕ' are *equivalent* if $m = m'$ is fulfilled and there exist an orientation-preserving diffeomorphism $h \colon \Sigma \to \Sigma$, integers $p, p' \in \mathbb{Z}_{\geq 0}$ and $c \in \mathbb{R}_{>0}$ such that $h(\tau_{n+p}, \mu_{n+p}) = (\tau'_{n'+p'}, c\mu'_{n'+p'})$. The condition for equivalent Agol cycles implies condition (2). See [6, Lemma 2.2].

Theorem 2.5 (Theorem 5.3 in Hodgson-Issa-Segerman [5])**.** *Pseudo-Anosov maps $\phi, \phi' \colon \Sigma \to \Sigma$ are conjugate in* $\mathrm{MCG}(\Sigma)$ *if and only if $\mathscr{P}$ and $\mathscr{P}'$ are combinatorially isomorphic.*

As a consequence, the equivalence class of an Agol cycle of ϕ is a conjugacy invariant. The Agol cycle length $\ell(\phi)$ and total splitting number $N(\phi)$ are conjugacy invariants as well, since they are equal for equivalent Agol cycles.

When we regard a maximal splitting $(\tau, \mu) \rightharpoonup (\tau', \mu')$ as an operation on the measured train track, we write $(\tau', \mu') = \rightharpoonup (\tau, \mu)$. We write n consecutive left (resp. right) maximal splittings $(\tau, \mu) \overset{\mathrm{l}}{\rightharpoonup}^n (\tau_n, \mu_n)$ (resp. $(\tau, \mu) \overset{\mathrm{r}}{\rightharpoonup}^n (\tau_n, \mu_n)$) as $(\tau_n, \mu_n) = \overset{\mathrm{l}}{\rightharpoonup}^n (\tau, \mu)$ (resp. $(\tau_n, \mu_n) = \overset{\mathrm{r}}{\rightharpoonup}^n (\tau, \mu)$). We also write a finite sequence $(\tau, \mu) \overset{\mathrm{l}}{\rightharpoonup}^n (\tau_n, \mu_n) \overset{\mathrm{r}}{\rightharpoonup}^m (\tau_{n+m}, \mu_{n+m})$ as $(\tau_{n+m}, \mu_{n+m}) = \overset{\mathrm{r}}{\rightharpoonup}^m \circ \overset{\mathrm{l}}{\rightharpoonup}^n (\tau, \mu)$.

The operation $\rightharpoonup$ and a diffeomorphism $\phi : \Sigma \to \Sigma$ commute on measured train tracks:

Lemma 2.6 (Lemma 2.1 in [6])**.** *Let (τ, μ) be a measured train track in Σ and $\phi : \Sigma \to \Sigma$ an orientation-preserving diffeomorphism. If (τ, μ) admits consecutive n left maximal splittings, then we have $(\phi \circ \overset{\mathrm{l}}{\rightharpoonup}^n)(\tau, \mu) = (\overset{\mathrm{l}}{\rightharpoonup}^n \circ \phi)(\tau, \mu)$. A parallel statement holds for $\overset{\mathrm{r}}{\rightharpoonup}^n$.*

Remark 2.7. (This remark is used for the proof of Theorem 5.1.) By Lemma 2.6 we have the following commutative diagram:

$$\begin{array}{ccccccc}
(\tau, \mu) & \rightharpoonup & (\tau_1, \mu_1) & \rightharpoonup & \cdots & \rightharpoonup & (\tau_n, \mu_n) \\
\downarrow & & \downarrow & & & & \downarrow \\
\phi(\tau, \mu) & \rightharpoonup & \phi(\tau_1, \mu_1) & \rightharpoonup & \cdots & \rightharpoonup & \phi(\tau_n, \mu_n)
\end{array}$$

Lemma 2.6 tells us that the (left, right, mixed) type of the maximal splitting $\phi(\tau_i, \mu_i) \rightharpoonup \phi(\tau_{i+1}, \mu_{i+1})$ is the same as that of $(\tau_i, \mu_i) \rightharpoonup (\tau_{i+1}, \mu_{i+1})$.

2.2. **Perron-Frobenius matrices.** We say that a matrix M is *positive* if each entry of M is positive. For matrices $A = (a_{rs})$ and $B = (b_{rs})$ with the same size, we write $A \geq B$ if $a_{rs} \geq b_{rs}$ for all r, s. Suppose that M is an n by n square matrix with nonnegative integer entries. We say that M is *Perron-Frobenius* if some power of M is a positive matrix. Perron-Frobenius matrices have the following properties.

Theorem 2.8 (Perron-Frobenius)**.** *A Perron-Frobenius M has a real eigenvalue $\lambda > 1$ which exceeds the moduli of all other eigenvalues. There exists a strictly positive eigenvector $\boldsymbol{v}$ associated with λ. Moreover, $\boldsymbol{v}$ is the unique positive eigenvector of M (up to positive multiples), and λ is a simple root of the characteristic equation of M.*

For the proof, see [4]. We call $\lambda = \lambda(M) > 1$ the *Perron-Frobenius eigenvalue* of M and call $\boldsymbol{v}$ a *Perron-Frobenius eigenvector.*

Definition 2.9. For each $n \in \mathbb{N}$ the subset $\mathcal{I}_n \subset \mathbb{N}_0^{3n}$ is defined as follows.

$$\mathcal{I}_n := \left\{ \boldsymbol{p} = (p_n, p_n', q_n, \dots, p_1, p_1', q_1) \in \mathbb{N}_0^{3n} \;\middle|\; \begin{array}{l} {}^\exists j,\ {}^\exists k \in \{1, \dots, n\} \text{ such that } p_j, p_k' > 0 \\ p_i + p_i', q_i > 0 \text{ for each } i \in \{1, \dots, n\} \end{array} \right\}$$

For example, $(1, 0, 2, 0, 1, 1) \in \mathcal{I}_2$, $(1, 0, 2, 1, 0, 1) \notin \mathcal{I}_2$. By definition, $\mathcal{I}_1 = \mathbb{N}^3$.

We recall the matrix $M_{\boldsymbol{p}} = M_1^{p_n} M_3^{p_n'} M_2^{q_n} \cdots M_1^{p_1} M_3^{p_1'} M_2^{q_1}$ for $\boldsymbol{p} \in \mathcal{I}_n$.

Lemma 2.10. *For each $\boldsymbol{p} \in \mathcal{I}_n$, $M_{\boldsymbol{p}}$ is Perron-Frobenius.*

Proof. A computation shows that $M_i^n \geq M_i \geq \left(\begin{smallmatrix} 1 & 0 & 0 \\ 0 & 1 & 0 \\ 0 & 0 & 1 \end{smallmatrix}\right)$ for $n \in \mathbb{N}$ and $i = 1, 2, 3$. By definition of $\mathcal{I}_n$, all the matrices M_1, M_2 and M_3 appear in the product $M_{\boldsymbol{p}}$ at least once. We can check that $M_{\boldsymbol{p}} \geq M_1 M_3 M_2 = M_3 M_1 M_2 > \mathbf{0}$. This means that $M_{\boldsymbol{p}}$ is positive. In particular, $M_{\boldsymbol{p}}$ is Perron-Frobenius. (This fact also follows from [9, Theorem 3.1].) $\square$

In this section we give an explicit description of a Perron-Frobenius eigenvector of $M_{\boldsymbol{p}}$ and its eigenvalue $\lambda_{\boldsymbol{p}}$. To do this, we first consider the infinite continued fraction expansion of an irrational number a.

$$a = a_0 + \cfrac{1}{a_1 + \cfrac{1}{\ddots + \cfrac{1}{a_k + \cdots}}} = [a_0, a_1, \cdots, a_k, \cdots]$$

with $a_i \in \mathbb{Z}$ and $a_i > 0$ for $i \geq 1$. By Lagrange's theorem, a is a quadratic irrational if and only if the expansion is eventually periodic; i.e., there exists $t \geq 1$ with $a_i = a_{i+t}$ for all $i \gg 1$. We write a quadratic irrational $a = [a_0, \cdots, a_{k-1}, b_0, \cdots, b_{t-1}, b_0, \cdots, b_{t-1}, \cdots]$ as $[a_0, \cdots, a_{k-1}, \overline{b_0, \cdots, b_{t-1}}]$.

Given $\boldsymbol{p} \in \mathcal{I}_n$, we next define the width $w_{\boldsymbol{p},j}$ and height $h_{\boldsymbol{p},j}$ for each $j \in \mathbb{N}_0$ as follows.

For $j = 0$, $w_{\boldsymbol{p},0} = 1$ and $h_{\boldsymbol{p},0} = [0, \overline{p_n + p'_n, q_n, ..., p_1 + p'_1, q_1}]$.

For $j > 0$, $w_{\boldsymbol{p},j} = w_{\boldsymbol{p},j-1} - (p_{n-j+1} + p'_{n-j+1}) h_{\boldsymbol{p},j-1}$ and $h_{\boldsymbol{p},j} = h_{\boldsymbol{p},j-1} - q_{n-j+1} w_{\boldsymbol{p},j}$.

The *split ratio* $s_{\boldsymbol{p}}$ $(0 < s_{\boldsymbol{p}} < 1)$ is defined by

$$s_{\boldsymbol{p}} = \sum_{i=0}^{\infty} p_{-i} h_{\boldsymbol{p},i},$$

where the index of p_{-i} is understood to be mod n.

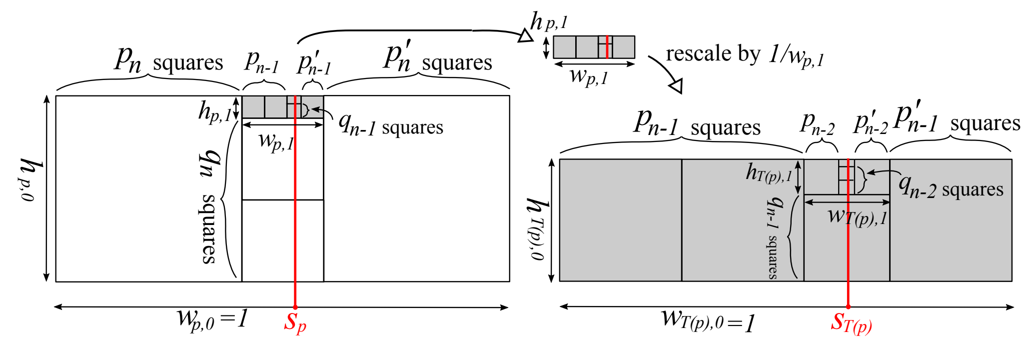

FIGURE 4. Partitioned rectangles (1) $\mathrm{rect}(\boldsymbol{p})$, (2) $\mathrm{rect}(T(\boldsymbol{p}))$ for $\boldsymbol{p} = (1, 1, 2, 2, 1, 1)$, $T(\boldsymbol{p}) = (2, 1, 1, 1, 1, 2) \in \mathcal{I}_2$.

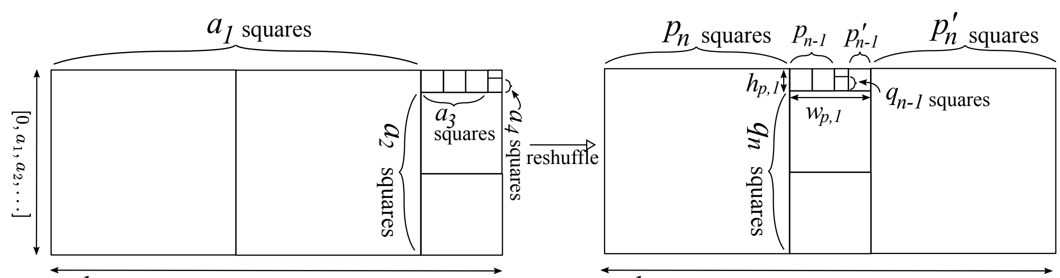

FIGURE 5. (1) Rectangle model for $[0, a_1, a_2, \ldots] = [0, 2, 2, 3, 1, \ldots]$. (2) Reshuffling squares when $[0, \overline{a_1, a_2, a_3, a_4}] = [0, \overline{1 + 1, 2, 2 + 1, 1}]$.

Definition 2.11. (Partitioned rectangle.) For $\boldsymbol{p} = (p_n, p'_n, q_n, ..., p_1, p'_1, q_1) \in \mathcal{I}_n$ we define a partitioned rectangle $\mathrm{rect}(\boldsymbol{p})$ as in Figure 4. We start out with a rectangle of width 1 and height $h_{\boldsymbol{p},0} = [0, \overline{p_n + p'_n, q_n, ..., p_1 + p'_1, q_1}]$. We then partition the rectangle into squares by the following procedure. First, we insert p_n squares from the left. In the remaining rectangle, we insert p'_n from the right and then q_n from the bottom. We do the same for $p_{n-1}, p'_{n-1}, q_{n-1}, \dots, p_1, p'_1, q_1, p_n, p'_n, q_n, \dots$, repeating the insertion pattern cyclically, infinitely many times. Rectangles for the example $\boldsymbol{p} = (1, 1, 2, 2, 1, 1)$ and $T(\boldsymbol{p})$ are illustrated in Figure 4.

Lemma 2.12. *The partitioned rectangle* $\mathrm{rect}(\boldsymbol{p})$ *is well defined.*

Proof. We introduce a useful tool for infinite continued fractions. (See also [7].) We define a rectangle whose width is 1 and whose height is $[0, a_1, a_2, \dots]$ for $a_i \in \mathbb{N}$. Then it is possible to iteratively fill in $a_1, a_2, \dots$ squares as in Figure 5(1). Suppose that $[0, \overline{a_1, a_2, \dots, a_{2n}}] = [0, \overline{p_n + p'_n, q_n, \dots, p_1 + p'_1, q_1}]$. We reshuffle the squares such that p_i squares are filled from the left and p'_i squares are filled from the right (see Figure 4). This shows that the partition into squares for $\boldsymbol{p} \in \mathcal{I}_n$ is well defined. $\square$

The values $w_{\boldsymbol{p},0}$, $h_{\boldsymbol{p},0}$ can be thought of as the widths and heights of the rectangles obtained when we iteratively delete outside squares as in Figure 4. The values are indicated in the picture.

Theorem 2.13. *For* $\boldsymbol{p} = (p_n, p'_n, q_n, \dots, p_1, p'_1, q_1) \in \mathcal{I}_n$ *the Perron-Frobenius eigenvalue* $\lambda_{\boldsymbol{p}}$ *of* $M_{\boldsymbol{p}}$ *and its eigenvector* $\boldsymbol{v} > \boldsymbol{0}$ *are given by*

$$\lambda_{\boldsymbol{p}} = \frac{1}{w_{\boldsymbol{p},n}} \quad \textit{and} \quad \boldsymbol{v} = \begin{pmatrix} s_{\boldsymbol{p}} \\ h_{\boldsymbol{p},0} \\ 1-s_{\boldsymbol{p}} \end{pmatrix}.$$

We call $\boldsymbol{v} = \boldsymbol{v_p}$ the *normalized eigenvector* with respect to $\lambda_{\boldsymbol{p}}$.

Proof. Recall that $T\colon \mathbb{N}_0^{3n} \to \mathbb{N}_0^{3n}$ is the shift as in Section 1. For $\boldsymbol{p} \in \mathcal{I}_n$ we define scaling factors $\lambda_{\boldsymbol{p},i} := w_{\boldsymbol{p},i}/w_{\boldsymbol{p},i+1}$ for $i \in \mathbb{N}_0$. The scaling factors fulfill the property $\prod_{i=0}^{n-1} \lambda_{\boldsymbol{p},i} = 1/w_{\boldsymbol{p},n}$. We will prove

$$\lambda_{\boldsymbol{p},0} M_2^{-q_n} M_1^{-p_n} M_3^{-p'_n} \begin{pmatrix} s_{\boldsymbol{p}} \\ h_{\boldsymbol{p},0} \\ 1-s_{\boldsymbol{p}} \end{pmatrix} = \begin{pmatrix} s_{T(\boldsymbol{p})} \\ h_{T(\boldsymbol{p}),0} \\ 1-s_{T(\boldsymbol{p})} \end{pmatrix}. \tag{2.1}$$

Using this, we can then inductively deduce the following statement:

$$\Big(\prod_{i=0}^{n-1} \lambda_{\boldsymbol{p},i}\Big)(M_1^{p_n} M_3^{p'_n} M_2^{q_n} \cdots M_1^{p_1} M_3^{p'_1} M_2^{q_1})^{-1} \begin{pmatrix} s_{\boldsymbol{p}} \\ h_{\boldsymbol{p},0} \\ 1-s_{\boldsymbol{p}} \end{pmatrix} = \begin{pmatrix} s_{T^n(\boldsymbol{p})} \\ h_{T^n(\boldsymbol{p}),0} \\ 1-s_{T^n(\boldsymbol{p})} \end{pmatrix} = \begin{pmatrix} s_{\boldsymbol{p}} \\ h_{\boldsymbol{p},0} \\ 1-s_{\boldsymbol{p}} \end{pmatrix} \tag{2.2}$$

The definitions of $w_{\boldsymbol{p},i}$ and $h_{\boldsymbol{p},i}$ are such that they line up with the lengths of the line segments in $\mathrm{rect}(\boldsymbol{p})$ as in Figure 4. Adding up the widths of all the squares on the left side, we get $s_{\boldsymbol{p}} (= \sum_{i=0}^{\infty} p_{-i} h_{\boldsymbol{p},i})$. Using Figure 4, we observe that for

$$\begin{pmatrix} y_1 \\ y_2 \\ y_3 \end{pmatrix} := M_2^{-q_n} M_1^{-p_n} M_3^{-p'_n} \begin{pmatrix} s_{\boldsymbol{p}} \\ h_{\boldsymbol{p},0} \\ 1-s_{\boldsymbol{p}} \end{pmatrix} = M_2^{-q_n} \begin{pmatrix} s_{\boldsymbol{p},0} - p_n h_{\boldsymbol{p},0} \\ h_{\boldsymbol{p},0} \\ 1-s_{\boldsymbol{p}} - p'_n h_{\boldsymbol{p},0} \end{pmatrix} = \begin{pmatrix} s_{\boldsymbol{p}} - p_n h_{\boldsymbol{p},0} \\ h_{\boldsymbol{p},0} - q_n(1-(p_n+p'_n)h_{\boldsymbol{p},0}) \\ 1-s_{\boldsymbol{p}} - p'_n h_{\boldsymbol{p},0} \end{pmatrix},$$

we have $w_{\boldsymbol{p},1} = 1 - (p_n + p'_n) h_{\boldsymbol{p},0} = y_1 + y_3$ and $h_{\boldsymbol{p},1} = h_{\boldsymbol{p},0} - q_n w_{\boldsymbol{p},1} = y_2$.

Remove $(p_n + p'_n)$ squares with height $h_{\boldsymbol{p},0}$ and q_n squares with height $w_{\boldsymbol{p},1}$ from $\mathrm{rect}(\boldsymbol{p})$. If we then scale the remaining small rectangle by $\lambda_{\boldsymbol{p},0} = 1/w_{\boldsymbol{p},1}$, its width becomes 1 and the rectangle becomes a partitioned rectangle. By moving all squares to the left, we see that its height must be $[0, \overline{p_{n-1}+p'_{n-1}, q_{n-1}, \ldots, p_1+p'_1, q_1, p_n+p'_n, q_n}] = h_{T(\boldsymbol{p}),0}$. Its partition into squares then tells us that the resulting partitioned rectangle is $\operatorname{rect}(T(\boldsymbol{p}))$. The value y_1 is the sum of the widths of all squares sitting on the left of the small rectangle. When scaling up y_1 by $\lambda_{\boldsymbol{p},0}$, the value $\lambda_{\boldsymbol{p},0} y_1$ continues to be the sum of square widths. This shows $\lambda_{\boldsymbol{p},0} y_1 = s_{T(\boldsymbol{p})}$. (See Figure 4.) This proves statement (2.1).

Statement (2.2) follows from applying statement (2.1) n times. The value $w_{\boldsymbol{p},n}^{-1} = \prod_{i=0}^{n-1} \lambda_{\boldsymbol{p},i}$ then becomes the eigenvalue of the eigenvector $\begin{pmatrix} s_{\boldsymbol{p}} \\ h_{\boldsymbol{p},0} \\ 1-s_{\boldsymbol{p}} \end{pmatrix}$ of $M_{\boldsymbol{p}}$. Because the vector entries are all positive and $M_{\boldsymbol{p}}$ is Perron-Frobenius, $w_{\boldsymbol{p},n}^{-1}$ must be the Perron-Frobenius eigenvalue $\lambda_{\boldsymbol{p}}$ by Theorem 2.8. □

Corollary 2.14. *The splitting ratio $s_{\boldsymbol{p}}$ can be written as follows.*

$$s_{\boldsymbol{p}} = \sum_{i=0}^{\infty} p_{-i} h_{\boldsymbol{p},i} = \frac{p_n h_{\boldsymbol{p},0} + p_{n-1} h_{\boldsymbol{p},1} + \cdots + p_1 h_{\boldsymbol{p},n-1}}{(p_n + p'_n) h_{\boldsymbol{p},0} + (p_{n-1} + p'_{n+1}) h_{\boldsymbol{p},1} + \cdots + (p_1 + p'_1) h_{\boldsymbol{p},n-1}}.$$

Proof. The split ratio $s_{\boldsymbol{p}}$ can be interpreted as a ratio dividing the width of the partitioned rectangle in two parts. Since the partitioned rectangle $\operatorname{rect}(\boldsymbol{p})$ is self-similar, it contains a rectangle that after rescaling by the factor $\lambda_{\boldsymbol{p}}$ is partitioned and equal to $\operatorname{rect}(\boldsymbol{p})$. To calculate $s_{\boldsymbol{p}}$, we can therefore ignore the width of the small self-similar rectangle and only use the ratio in the statement instead. □

Remark 2.15. For $\boldsymbol{p} \in \mathcal{I}_n$ the height $h_{\boldsymbol{p},0}$ is a quadratic irrational since the continued fraction expansion is eventually periodic. One can prove inductively that the width $w_{\boldsymbol{p},j}$ is a quadratic irrational for each $j \in \mathbb{N}_0$. Thus $\lambda_{\boldsymbol{p}} = w_{\boldsymbol{p},n}^{-1}$ is also a quadratic irrational.

Corollary 2.16. *Let $\boldsymbol{p} = (p_n, p'_n, q_n, \ldots, p_1, p'_1, q_1) \in \mathcal{I}_n$ and $\boldsymbol{t} = (t_n, t'_n, u_n, \ldots, t_1, t'_1, u_1) \in \mathcal{I}_n$. If $p_i + p'_i = t_i + t'_i$ and $q_i = u_i$ hold for all $i \in \{1, \ldots, n\}$, then we have the following.*

(1) $\lambda_{\boldsymbol{p}} = \lambda_{\boldsymbol{t}}$.
(2) *If $\boldsymbol{t} = f(\boldsymbol{p})$, then $s_{\boldsymbol{p}} + s_{f(\boldsymbol{p})} = 1$, where $f : \mathbb{N}_0^{3n} \to \mathbb{N}_0^{3n}$ is the flip.*
(3) *If $(p_n, p_{n-1}, \ldots, p_1) \prec (t_n, t_{n-1}, \ldots, t_1)$, then $s_{\boldsymbol{p}} < s_{\boldsymbol{t}}$, where $\prec$ is the lexicographic ordering of $\mathbb{N}_0^n$.*

Proof. Claim (1) follows from Theorem 2.13 since $w_{\boldsymbol{p},n} = w_{\boldsymbol{t},n}$ holds for all $n \in \mathbb{N}_0$. Exchanging p_i and p'_i for all $i \in \{1, ..., n\}$, flips the partitioned rectangle $\operatorname{rect}(\boldsymbol{p})$ horizontally. This means that $s_{f(\boldsymbol{p})} = 1 - s_{\boldsymbol{p}}$. The proof of (2) is done. For each $\boldsymbol{p} \in \mathcal{I}_n$ and all $i \in \mathbb{N}_0$, we have the property $w_{\boldsymbol{p},i+1} < h_{\boldsymbol{p},i}$. Using the definition of the partitioned rectangle, this implies claim (3). □

For a vector $\boldsymbol{v} = (v_i) \in \mathbb{R}^n$, we denote by $\boldsymbol{v}|_i$ the i-th coordinate v_i of $\boldsymbol{v}$. When M is an n by n square matrix, we also use the symbol $M\boldsymbol{v}|_i$ which returns the i-th coordinate of the vector $M\boldsymbol{v}$.

Corollary 2.17. *For $\boldsymbol{p} \in \mathcal{I}_n$ let $\boldsymbol{v} > \mathbf{0}$ be a Perron-Frobenius eigenvector of $M_{\boldsymbol{p}}$. Then $\boldsymbol{v}|_1 = \boldsymbol{v}|_3$ holds if and only if $\boldsymbol{p}$ is symmetric.*

Proof. Corollary 2.16(2)(3) implies that $s_{\boldsymbol{p}} = \frac{1}{2}$ holds if and only if $f(\boldsymbol{p}) = \boldsymbol{p}$ holds; i.e., $\boldsymbol{p}$ is symmetric. By Theorem 2.13 the Perron-Frobenius eigenvector $\boldsymbol{v} = \boldsymbol{v}_{\boldsymbol{p}}$ satisfies the desired property. $\square$

Example 2.18. Let us apply Theorem 2.13 and Corollary 2.14 to compute $s_{\boldsymbol{p}}$ and $\lambda_{\boldsymbol{p}}$.

(1) Let $\boldsymbol{p} = (p, p', q) \in \mathcal{I}_1$. Then $h_{\boldsymbol{p},0} = [0, \overline{p+p', q}\,]$. We have
$$s_{\boldsymbol{p}} = \frac{p h_{\boldsymbol{p},0}}{(p+p')h_{\boldsymbol{p},0}} = \frac{p}{p+p'}, \qquad \lambda_{\boldsymbol{p}} = \frac{1}{w_{\boldsymbol{p},1}} = \frac{1}{1-(p+p')h_{\boldsymbol{p},0}}.$$

(2) Let $\boldsymbol{p} = (1,0,1,0,1,1) \in \mathcal{I}_2$. We have $h_{\boldsymbol{p},0} = [0, \overline{1}\,] = \frac{-1+\sqrt{5}}{2}$, $w_{\boldsymbol{p},1} = 1 - h_{\boldsymbol{p},0}$, $h_{\boldsymbol{p},1} = h_{\boldsymbol{p},0} - w_{\boldsymbol{p},1}$, and $w_{\boldsymbol{p},2} = w_{\boldsymbol{p},1} - h_{\boldsymbol{p},1}$. Hence, $s_{\boldsymbol{p}}$ and $\lambda_{\boldsymbol{p}}$ are given by
$$s_{\boldsymbol{p}} = \frac{h_{\boldsymbol{p},0}}{h_{\boldsymbol{p},0} + h_{\boldsymbol{p},1}} = \frac{h_{\boldsymbol{p},0}}{3h_{\boldsymbol{p},0} - 1}, \qquad \lambda_{\boldsymbol{p}} = \frac{1}{w_{\boldsymbol{p},2}} = \frac{1}{2 - 3h_{\boldsymbol{p},0}} = \frac{7+3\sqrt{5}}{2}.$$

By a calculation we have the following lemma.

Lemma 2.19. *Let $q \in \mathbb{N}$ and $p, p' \in \mathbb{N}_0$. Let $\boldsymbol{x} = \left(\begin{smallmatrix} x \\ y \\ z \end{smallmatrix}\right) > \mathbf{0}$.*

(1) *$M_1^p M_3^p M_2^q \boldsymbol{x}|_1 \le M_1^p M_3^p M_2^q \boldsymbol{x}|_3$ if and only if $x \le z$.*
(2) *Suppose that $p > p' \ge 0$. Then $M_1^p M_3^{p'} M_2^q \boldsymbol{x}|_1 > M_1^p M_3^{p'} M_2^q \boldsymbol{x}|_3$ for any $\boldsymbol{x} > \mathbf{0}$.*
(3) *Suppose that $0 \le p < p'$. Then $M_1^p M_3^{p'} M_2^q \boldsymbol{x}|_1 < M_1^p M_3^{p'} M_2^q \boldsymbol{x}|_3$ for any $\boldsymbol{x} > \mathbf{0}$.*

As a corollary of Lemma 2.19, we immediately have the following result.

Corollary 2.20. *If $\boldsymbol{x} = \left(\begin{smallmatrix} x \\ y \\ z \end{smallmatrix}\right)$ is a positive vector with $x \ne z$, then $M_1^p M_3^{p'} M_2^q \boldsymbol{x}|_1 \ne M_1^p M_3^{p'} M_2^q \boldsymbol{x}|_3$ for any $q \in \mathbb{N}$ and $p, p' \in \mathbb{N}_0$ (possibly $p = p'$).*

2.3. **Pseudo-Anosov maps in the semigroup $F_D = F(\sigma_1, \sigma_3, \sigma_2^{-1})$.** We write $h_1 = \sigma_1$, $h_3 = \sigma_3$ and $h_2 = \sigma_2^{-1}$. For a map $h = h_{n_k} \cdots h_{n_1} \in F_D$ ($n_i \in \{1,2,3\}$) we set $M_h := M_{n_k} \cdots M_{n_1}$. The following is a well-known result.

Proposition 2.21. *The product $h = h_{n_k} \cdots h_{n_1} \in F_D$ is pseudo-Anosov if all σ_1, σ_3 and σ_2^{-1} appear in the product at least once. In this case the dilatation $\lambda(h)$ of h equals the Perron-Frobenius eigenvalue $\lambda(M_h)$.*

For the convenience of the reader, we give an outline of the proof. We use a criterion by Bestvina-Handel algorithm [3] to determine when a mapping class is pseudo-Anosov. We first choose a finite graph $G \subset \Sigma_{0,5}$ that is homotopy equivalent to $\Sigma_{0,5}$ as in Figure 6(2). The graph G has four vertices $1, \ldots, 4$ and four loop edges, each of which encircles a puncture. Let P be the set of four loop edges of G.

Given a mapping class $\psi \in \mathrm{MCG}(\Sigma_{0,5})$, one can pick an induced graph map $g : G \to G$ homotopic to ψ. We require that g sends vertices to vertices, edges to edge paths and fulfills $g(P) = P$. (See [3, Section 1].) We may suppose that g has no backtracks; i.e., g maps each oriented edge of G to an edge path which does not contain an oriented edge e followed by the same edge $\bar{e}$ with the opposite orientation. This map g defines a 3 by 3 *transition matrix* M (with respect to the 3 non-loop edges). For $r, s \in \{1, 2, 3\}$ the entry M_{rs} is the number of times that the g-image of the s-th edge runs the r-th edge in either direction. We say that $g : G \to G$ is *efficient* if $g^n : G \to G$ has no backtracks for all $n > 0$.

Notice that h_i for $i \in \{1, 2, 3\}$ induces a graph map $g_i : G \to G$ which has no backtracks as shown Figure 6(1)–(4). The transition matrix of g_i is given by the matrix M_i as in Section 1.

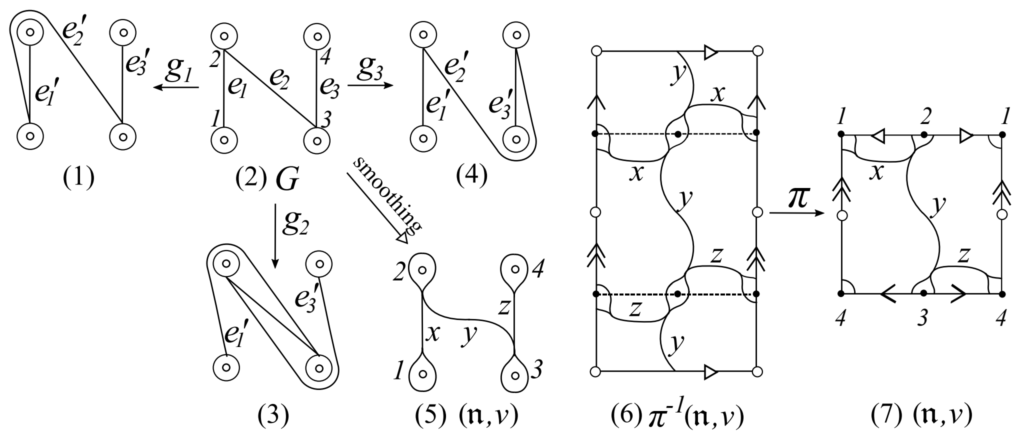

FIGURE 6. (1)–(4) The graph maps $g_i : G \to G$. $e_j' := g_i(e_j)$. (5) $(\mathfrak{n}, \boldsymbol{v} = \begin{pmatrix} x \\ y \\ z \end{pmatrix})$ in $\Sigma_{0,5}$. (6)(7) The 2-fold branched cover $\pi\colon \Sigma_{1,2} \to \Sigma_{0,5}$.

The composition $g_h := g_{n_k} \cdots g_{n_1} : G \to G$ is an induced graph map of $h = h_{n_k} \cdots h_{n_1}$. (A priori, g_h could have backtracks.) We call k the length of the graph map g_h. By induction on the length k, it can be shown that $g_h : G \to G$ has no backtracks for any $h \in F_D$. In particular, $g_h^n : G \to G$ has no backtracks for any $n > 0$; i.e., $g_h : G \to G$ is efficient, because g_h^n is an induced graph map of $h^n \in F_D$. Since $g_h : G \to G$ has no backtracks, the transition matrix with respect to the non-loop edges of g_h is given by M_h. If all σ_1, σ_3 and σ_2^{-1} appear in the product h at least once, then M_h is Perron-Frobenius by Lemma 2.10. By the Bestvina-Handel algorithm [3], the two conditions ($g_h : G \to G$ is efficient, and the transition matrix M_h is Perron-Frobenius) ensure that h is pseudo-Anosov with dilatation $\lambda(M_h)$.

Remark 2.22. Let $g_h : G \to G$ be an efficient graph map. We obtain a trivalent train track $\mathfrak{n}$ in $\Sigma_{0,5}$ (Figure 6(5)) by *graph smoothing* near the vertices of G. See [3, Section 3.3] for more details. Denote by $\boldsymbol{v}$ the Perron-Frobenius eigenvector of M_h. We assign the weight

$\boldsymbol{v}|_i$ (that is the i-th coordinate of $\boldsymbol{v}$) to the i-th branch and we obtain the measured train track $(\mathfrak{n}, \boldsymbol{v})$ (also described in Figure 6(5)). This measured train track $(\mathfrak{n}, \boldsymbol{v})$ is suited to the stable measured lamination of h by [3, Section 3.4].

2.4. **Pseudo-Anosov maps in the semigroup** $F_T = F(\delta_1, \delta_3, \delta_2^{-1})$**.** The union of curves $c_1 \cup c_2 \cup c_3$ (Figure 2(1)) fills the surface $\Sigma_{1,2}$. A construction of pseudo-Anosov maps by Penner [9, Theorem 3.1] tells us that the product of δ_1, δ_3 and δ_2^{-1} is pseudo-Anosov if all the Dehn twists δ_1, δ_3 and δ_2^{-1} appear in the product at least once. Thus for each $\boldsymbol{p} \in \mathcal{I}_n$, the map $\Phi_{\boldsymbol{p}} \in F_T$ is pseudo-Anosov by the definition of $\mathcal{I}_n$ (Definition 2.9). The map $\phi_{\boldsymbol{p}} \in F_D$ is also pseudo-Anosov for each $\boldsymbol{p} \in \mathcal{I}_n$ by Proposition 2.21. Additionally, each pseudo-Anosov map in F_T (resp. F_D) is conjugate to $\Phi_{\boldsymbol{p}}$ (resp. $\phi_{\boldsymbol{p}}$) for some $\boldsymbol{p} \in \mathcal{I}_n$. The link between the maps $\Phi_{\boldsymbol{p}}$ and $\phi_{\boldsymbol{p}}$ can be found in the following lemma.

Lemma 2.23. *For $\boldsymbol{p} \in \mathcal{I}_n$ let $\boldsymbol{v} > \boldsymbol{0}$ be an eigenvector for the Perron-Frobenius eigenvalue $\lambda_{\boldsymbol{p}}$ of $M_{\boldsymbol{p}}$. Then the measured train tracks $(\mathfrak{b}_L, \boldsymbol{v})$ in $\Sigma_{0,5}$ and $(\mathfrak{b}, \boldsymbol{v})$ in $\Sigma_{1,2}$ defined in Section 1 are suited to the stable measured laminations of $\phi_{\boldsymbol{p}} \in F_D$ and $\Phi_{\boldsymbol{p}} \in F_T$ respectively. Moreover, it holds $\lambda(\phi_{\boldsymbol{p}}) = \lambda(\Phi_{\boldsymbol{p}}) = \lambda_{\boldsymbol{p}}$, where $\lambda_{\boldsymbol{p}}$ is a quadratic irrational.*

Proof. By Remark 2.22 $(\mathfrak{n}, 2\boldsymbol{v})$ is suited to the stable measured lamination of $\phi_{\boldsymbol{p}}$. Figure 7 illustrates that $(\mathfrak{n}, 2\boldsymbol{v})$ is equivalent to $(\mathfrak{b}_L, \boldsymbol{v})$. Therefore, $(\mathfrak{b}_L, \boldsymbol{v})$ is also suited to the stable measured lamination of $\phi_{\boldsymbol{p}}$.

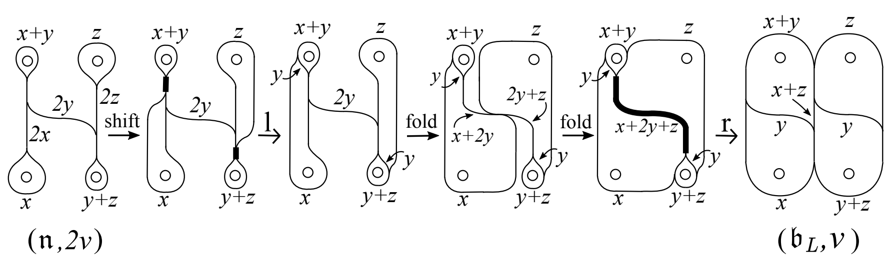

FIGURE 7. $\xrightarrow{l}$ (resp. $\xrightarrow{r}$) denotes the left (resp. right) splittings at the highlighted large branches. $(\mathfrak{n}, 2\boldsymbol{v})$ is equivalent to $(\mathfrak{b}_L, \boldsymbol{v})$.

We regard $\Sigma_{0,5}$ as the once punctured sphere with four marked points p_i ($i \in \{1, \dots, 4\}$). Consider a 2-fold branched cover $\pi \colon \Sigma_{1,2} \to \Sigma_{0,5}$ branched over the four marked points and induced by the hyperelliptic involution of $\Sigma_{1,2}$, exchanging the two punctures. Notice that $\delta_j := \delta_{c_j} \in \mathrm{MCG}(\Sigma_{1,2})$ is a lift of $\sigma_j \in \mathrm{MCG}(\Sigma_{0,5})$. Hence, $\Phi_{\boldsymbol{p}} \in F_T$ is a lift of $\phi_p \in F_D$. It follows that $\Phi_{\boldsymbol{p}}$ and $\phi_{\boldsymbol{p}}$ have the same dilatation. By Proposition 2.21 we have $\lambda(\phi_{\boldsymbol{p}}) = \lambda_{\boldsymbol{p}}$. Thus $\lambda(\Phi_{\boldsymbol{p}}) = \lambda(\phi_{\boldsymbol{p}}) = \lambda_{\boldsymbol{p}}$. By Remark 2.15 $\lambda_{\boldsymbol{p}}$ is a quadratic irrational.

Let $\mathcal{F}^s$ and $\mathcal{F}^u$ be the stable and unstable foliations with respect to $\phi_{\boldsymbol{p}}$. The preimages $\pi^{-1}(\mathcal{F}^s)$ and $\pi^{-1}(\mathcal{F}^u)$ give the stable and unstable foliations with respect to $\Phi_{\boldsymbol{p}}$. Since p_i is a 1-pronged singular point of $\mathcal{F}^s$ and $\mathcal{F}^u$, the preimage $\pi^{-1}(p_i)$ is a regular point (i.e., a 2-pronged point) of $\pi^{-1}(\mathcal{F}^s)$ and $\pi^{-1}(\mathcal{F}^u)$. Notice that $\pi^{-1}(\mathfrak{n})$ admits four bigons each of which contains a regular point $\pi^{-1}(p_i)$. See Figure 6(6)(7). Then the measured train track $(\mathfrak{b}, \boldsymbol{v})$ in $\Sigma_{1,2}$ is obtained from $\pi^{-1}(\mathfrak{n}, \boldsymbol{v})$ by collapsing each bigon. As a result, $(\mathfrak{b}, \boldsymbol{v})$ is suited to the stable measured lamination of $\Phi_{\boldsymbol{p}}$. $\square$

We will choose $(\mathfrak{b}, \lambda_{\boldsymbol{p}}\boldsymbol{v})$ (resp. $(\mathfrak{b}_L, \lambda_{\boldsymbol{p}}\boldsymbol{v})$) as the start of the maximal splitting sequence in the proof of Theorem 1.2 (resp. Theorem 4.1).

3. Agol cycles of pseudo-Anosov maps in F_T

The goal of this section is to prove Theorem 1.2. To do this, we first construct finite sequences of maximal splittings (Lemma 3.1, Proposition 3.2). Then we concatenate some finite sequences to produce an Agol cycle of the pseudo-Anosov map $\Phi_{\boldsymbol{p}}$.

When $\boldsymbol{p}$ is symmetric, the normalized eigenvector $\boldsymbol{v}_{\boldsymbol{p}}$ with respect to $\lambda_{\boldsymbol{p}}$ fulfills $\boldsymbol{v}_{\boldsymbol{p}}|_1 = \boldsymbol{v}_{\boldsymbol{p}}|_3$ (Corollary 2.17). This extra symmetry gives simpler maximal splitting sequences. Hence, the measured train tracks with symmetric weights (i.e. $x = z$) and asymmetric weights (i.e. $x \neq z$) will be treated differently in the following lemma.

Lemma 3.1. *Let $q \in \mathbb{N}$ and $p, p' \in \mathbb{N}_0$. Let $\boldsymbol{x} = \begin{pmatrix} x \\ y \\ z \end{pmatrix} > \boldsymbol{0}$.*

(1) *Suppose that $p > 0$. Then*
$$(\mathfrak{b}, M_1^{p-1}M_3^{p-1}M_2^q\boldsymbol{x}) = \begin{cases} (\delta_1^{-1}\delta_3^{-1} \circ \overset{\mathrm{r}}{\rightharpoondown})(\mathfrak{b}, M_1^pM_3^pM_2^q\boldsymbol{x}) & \text{if } x = z, \\ (\delta_1^{-1}\delta_3^{-1} \circ \overset{\mathrm{r}}{\rightharpoondown}{}^2)(\mathfrak{b}, M_1^pM_3^pM_2^q\boldsymbol{x}) & \text{if } x \neq z. \end{cases}$$

(2) *Suppose that $p > p' \geq 0$. Then*
$$(\mathfrak{b}, M_1^{p-1}M_3^{p'}M_2^q\boldsymbol{x}) = (\delta_1^{-1} \circ \overset{\mathrm{r}}{\rightharpoondown})(\mathfrak{b}, M_1^pM_3^{p'}M_2^q\boldsymbol{x}).$$

(3) *Suppose that $0 \leq p < p'$. Then*
$$(\mathfrak{b}, M_1^pM_3^{p'-1}M_2^q\boldsymbol{x}) = (\delta_3^{-1} \circ \overset{\mathrm{r}}{\rightharpoondown})(\mathfrak{b}, M_1^pM_3^{p'}M_2^q\boldsymbol{x}).$$

(4) $$(\mathfrak{b}, M_2^{q-1}\boldsymbol{x}) = \begin{cases} (\delta_2 \circ \overset{1}{\rightharpoondown}{}^2)(\mathfrak{b}, M_2^q\boldsymbol{x}) & \text{if } x = z, \\ (\delta_2 \circ \overset{1}{\rightharpoondown}{}^3)(\mathfrak{b}, M_2^q\boldsymbol{x}) & \text{if } x \neq z. \end{cases}$$

Proof. A calculation $M_2^q\boldsymbol{x} = \begin{pmatrix} x \\ qx+y+qz \\ z \end{pmatrix}$ shows that $\boldsymbol{x}|_1 = M_2^q\boldsymbol{x}|_1 = x$ and $\boldsymbol{x}|_3 = M_2^q\boldsymbol{x}|_3 = z$. For the proof of claims (1)–(4), it is suffices to prove them for $q = 1$. In fact, once we prove claims (1)–(4) for $q = 1$, we can apply them to the positive vector $\boldsymbol{x}' = M_2^{q-1}\boldsymbol{x}$.

We have $M_1^pM_3^pM_2\begin{pmatrix} x \\ y \\ z \end{pmatrix} = \begin{pmatrix} x+py' \\ y' \\ py'+z \end{pmatrix}$, where $y' = x + y + z$. The measured train track $(\tau_0, \mu_0) := (\mathfrak{b}, M_1^pM_3^pM_2\boldsymbol{x})$ has two large branches with weights $x+(p+1)y'$ and $(p+1)y'+z$.

We first consider the case $x \neq z$. We may suppose that $x < z$. Applying 2 maximal splittings (see Figure 8), we obtain 2 right maximal splittings

$$(\tau_0, \mu_0) = (\mathfrak{b}, M_1^p M_3^p M_2 \boldsymbol{x}) \overset{\mathrm{r}}{\rightharpoondown}{}^2 (\tau_2, \mu_2) = \delta_1 \delta_3 (\mathfrak{b}, M_1^{p-1} M_3^{p-1} M_2 \boldsymbol{x}).$$

In other words, $(\mathfrak{b}, M_1^{p-1} M_3^{p-1} M_2 \boldsymbol{x}) = (\delta_1^{-1} \delta_3^{-1} \circ \overset{\mathrm{r}}{\rightharpoondown}{}^2)(\mathfrak{b}, M_1^p M_3^p M_2 \boldsymbol{x})$. This gives claim (1) when $x < z$.

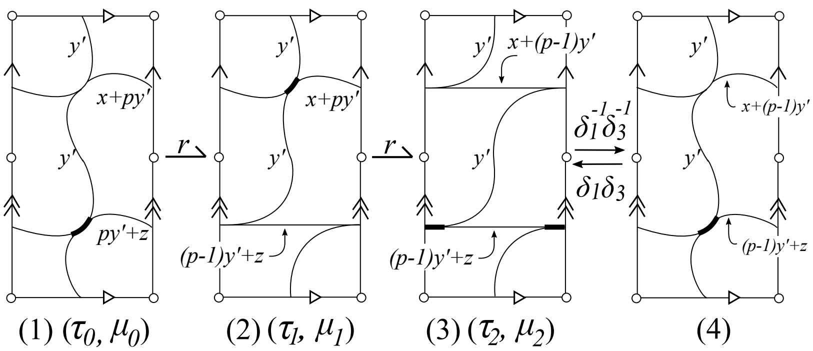

FIGURE 8. Proof of Lemma 3.1(1) when $x < z$. (1) $(\mathfrak{b}, M_1^p M_3^p M_2 \boldsymbol{x})$. (4) $(\mathfrak{b}, M_1^{p-1} M_3^{p-1} M_2 \boldsymbol{x})$.

In the case $x = z$, the two large branches of the measured train track $(\mathfrak{b}, M_1^p M_3^p M_2 \boldsymbol{x})$ have the same maximal weight. Applying the maximal splitting, we obtain the right maximal splitting

$$(\tau_0, \mu_0) = (\mathfrak{b}, M_1^p M_3^p M_2 \boldsymbol{x}) \overset{\mathrm{r}}{\rightharpoondown} (\tau_1, \mu_1) = \delta_1 \delta_3 (\mathfrak{b}, M_1^{p-1} M_3^{p-1} M_2 \boldsymbol{x}).$$

This completes the proof of claim (1).

We turn to claim (2). Suppose that $p > p' \geq 0$. We have $M_1^p M_3^{p'} M_2 \begin{pmatrix} x \\ y \\ z \end{pmatrix} = \begin{pmatrix} x+py' \\ y' \\ p'y'+z \end{pmatrix}$, where $y' = x + y + z$. By a calculation we have $M_1^p M_3^{p'} M_2 \boldsymbol{x}|_1 = x + py' > M_1^p M_3^{p'} M_2 \boldsymbol{x}|_3 = p'y' + z$. The measured train track $(\tau_0, \mu_0) := (\mathfrak{b}, M_1^p M_3^{p'} M_2 \boldsymbol{x})$ has two large branches with weights $x + (p+1)y'$ and $(p'+1)y' + z$. Applying a maximal splitting (see Figure 9), we obtain a right maximal splitting

$$(\tau_0, \mu_0) = (\mathfrak{b}, M_1^p M_3^{p'} M_2 \boldsymbol{x}) \overset{\mathrm{r}}{\rightharpoondown} (\tau_1, \mu_1) = \delta_1 (\mathfrak{b}, M_1^{p-1} M_3^{p'} M_2 \boldsymbol{x}).$$

The proof of claim (2) is done. One can prove claim (3) in a similar way.

We now prove claim (4). We set $(\tau_0, \mu_0) = \left(\mathfrak{b}, M_2 \boldsymbol{x} = \begin{pmatrix} x \\ x+y+z \\ z \end{pmatrix}\right)$. Consider the case $x \neq z$. We may suppose that $x < z$. Applying 3 maximal splittings (see Figure 10), we obtain 3 left maximal splittings

$$(\tau_0, \mu_0) = (\mathfrak{b}, M_2 \boldsymbol{x}) \overset{\mathrm{l}}{\rightharpoondown} (\tau_1, \mu_1) \overset{\mathrm{l}}{\rightharpoondown} (\tau_2, \mu_2) \overset{\mathrm{l}}{\rightharpoondown} (\tau_3, \mu_3) = \delta_2^{-1} (\mathfrak{b}, \boldsymbol{x}).$$

This gives claim (4) for $x < z$.

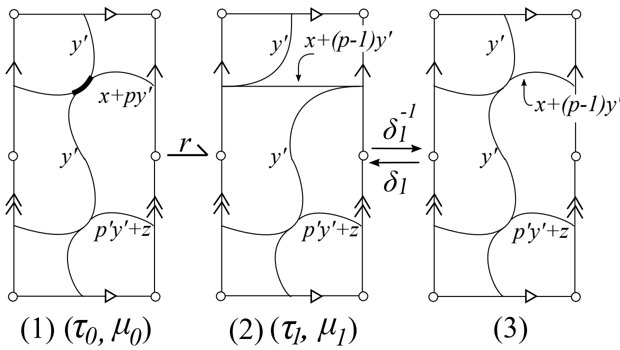

FIGURE 9. Proof of Lemma 3.1(2). (1) $(\mathfrak{b}, M_1^p M_3^{p'} M_2\boldsymbol{x})$. (3) $(\mathfrak{b}, M_1^{p-1} M_3^{p'} M_2\boldsymbol{x})$.

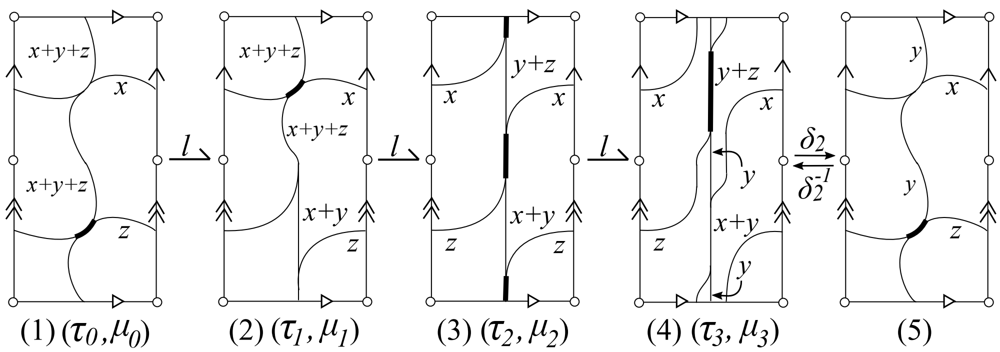

FIGURE 10. Proof of Lemma 3.1(4) when $x < z$. (1) $(\mathfrak{b}, M_2\boldsymbol{x})$. (5) $(\mathfrak{b}, \boldsymbol{x})$.

In the case $x = z$, the two large branches of $(\mathfrak{b}, M_2\boldsymbol{x})$ have the same maximal weight. Applying 2 maximal splittings, we obtain 2 left maximal splittings $(\mathfrak{b}, M_2\boldsymbol{x}) \overset{\mathrm{l}}{\rightharpoondown}{}^{2}\, \delta_2^{-1}(\mathfrak{b}, \boldsymbol{x})$. This completes the proof. $\square$

Proposition 3.2. *Let $q \in \mathbb{N}$ and $p, p' \in \mathbb{N}_0$. Let $\boldsymbol{x} = \left(\begin{smallmatrix} x \\ y \\ z \end{smallmatrix}\right) > \mathbf{0}$.*

(1) *(Symmetric case.) Suppose that $p > 0$. Then*

$$(\mathfrak{b}, \boldsymbol{x}) = (\delta_2^q \delta_1^{-p} \delta_3^{-p} \circ \overset{\mathrm{l}}{\rightharpoondown}{}^{2q} \circ \overset{\mathrm{r}}{\rightharpoondown}{}^{p})(\mathfrak{b}, M_1^p M_3^p M_2^q \boldsymbol{x}) \ \text{ if } x = z.$$

(2) *(Asymmetric case.) Suppose that $p + p' > 0$ (possibly $p = p' > 0$). Then*

$$(\mathfrak{b}, \boldsymbol{x}) = (\delta_2^q \delta_1^{-p} \delta_3^{-p'} \circ \overset{\mathrm{l}}{\rightharpoondown}{}^{3q} \circ \overset{\mathrm{r}}{\rightharpoondown}{}^{p+p'})(\mathfrak{b}, M_1^p M_3^{p'} M_2^q \boldsymbol{x}) \ \text{ if } x \neq z.$$

Proof. We first prove claim (2) in the special case $p = p' > 0$. Applying Lemma 3.1(1) in the latter case $x \neq z$, we have

$$(\mathfrak{b}, M_1^{p-1} M_3^{p-1} M_2^q \boldsymbol{x}) = ((\delta_1\delta_3)^{-1} \circ \overset{\mathrm{r}}{\rightharpoonup}^{2})(\mathfrak{b}, M_1^p M_3^p M_2^q \boldsymbol{x}). \tag{3.1}$$

Then applying Lemma 3.1(1) again, we obtain

$$\begin{aligned}
(\mathfrak{b}, M_1^{p-2} M_3^{p-2} M_2^q \boldsymbol{x}) &= ((\delta_1\delta_3)^{-1} \circ \overset{\mathrm{r}}{\rightharpoonup}^{2})(\mathfrak{b}, M_1^{p-1} M_3^{p-1} M_2^q \boldsymbol{x}) \\
&= ((\delta_1\delta_3)^{-1} \circ \overset{\mathrm{r}}{\rightharpoonup}^{2}) \circ ((\delta_1\delta_3)^{-1} \circ \overset{\mathrm{r}}{\rightharpoonup}^{2})(\mathfrak{b}, M_1^p M_3^p M_2^q \boldsymbol{x}) \quad (\because (3.1)) \\
&= ((\delta_1\delta_3)^{-2} \circ \overset{\mathrm{r}}{\rightharpoonup}^{4})(\mathfrak{b}, M_1^p M_3^p M_2^q \boldsymbol{x}). \quad (\because \text{Lemma 2.6}).
\end{aligned}$$

Repeating this argument, we have

$$(\mathfrak{b}, M_2^q \boldsymbol{x}) = ((\delta_1\delta_3)^{-p} \circ \overset{\mathrm{r}}{\rightharpoonup}^{2p})(\mathfrak{b}, M_1^p M_3^p M_2^q \boldsymbol{x}). \tag{3.2}$$

Applying Lemma 3.1(4) in the case $x \neq z$ repeatedly, we have

$$(\mathfrak{b}, \boldsymbol{x}) = (\delta_2^q \circ \overset{1}{\rightharpoonup}^{3q})(\mathfrak{b}, M_2^q \boldsymbol{x}). \tag{3.3}$$

The above equalities (3.2) and (3.3) give us

$$\begin{aligned}
(\mathfrak{b}, \boldsymbol{x}) &= (\delta_2^q \circ \overset{1}{\rightharpoonup}^{3q})(\mathfrak{b}, M_2^q \boldsymbol{x}) \quad (\because (3.3)) \\
&= (\delta_2^q \circ \overset{1}{\rightharpoonup}^{3q}) \circ ((\delta_1\delta_3)^{-p} \circ \overset{\mathrm{r}}{\rightharpoonup}^{2p})(\mathfrak{b}, M_1^p M_3^p M_2^q \boldsymbol{x}) \quad (\because (3.2)) \\
&= (\delta_2^q \delta_1^{-p} \delta_3^{-p} \circ \overset{1}{\rightharpoonup}^{3q} \circ \overset{\mathrm{r}}{\rightharpoonup}^{2p})(\mathfrak{b}, M_1^p M_3^p M_2^q \boldsymbol{x}). \quad (\because \text{Lemma 2.6},\ \delta_1\delta_3 = \delta_3\delta_1)
\end{aligned}$$

This is the desired equality in the case $p = p'$. Next we prove claim (2) in the general case. We may suppose that $0 \leq p < p'$. Applying Lemma 3.1(3) repeatedly, we have

$$(\mathfrak{b}, M_1^p M_3^p M_2^q \boldsymbol{x}) = (\delta_3^{-(p'-p)} \circ \overset{\mathrm{r}}{\rightharpoonup}^{p'-p})(\mathfrak{b}, M_1^p M_3^{p'} M_2^q \boldsymbol{x}). \tag{3.4}$$

This together with the equalities (3.2) and (3.3) implies that

$$\begin{aligned}
(\mathfrak{b}, \boldsymbol{x}) &= (\delta_2^q \circ \overset{1}{\rightharpoonup}^{3q})(\mathfrak{b}, M_2^q \boldsymbol{x}) \quad (\because (3.3)) \\
&= (\delta_2^q \circ \overset{1}{\rightharpoonup}^{3q}) \circ ((\delta_1\delta_3)^{-p} \circ \overset{\mathrm{r}}{\rightharpoonup}^{2p})(\mathfrak{b}, M_1^p M_3^p M_2^q \boldsymbol{x}) \quad (\because (3.2)) \\
&= (\delta_2^q \circ \overset{1}{\rightharpoonup}^{3q}) \circ ((\delta_1\delta_3)^{-p} \circ \overset{\mathrm{r}}{\rightharpoonup}^{2p}) \circ (\delta_3^{-(p'-p)} \circ \overset{\mathrm{r}}{\rightharpoonup}^{p'-p})(\mathfrak{b}, M_1^p M_3^{p'} M_2^q \boldsymbol{x}) \quad (\because (3.4)) \\
&= (\delta_2^q \delta_1^{-p} \delta_3^{-p'} \circ \overset{1}{\rightharpoonup}^{3q} \circ \overset{\mathrm{r}}{\rightharpoonup}^{p+p'})(\mathfrak{b}, M_1^p M_3^{p'} M_2^q \boldsymbol{x}) \quad (\because \text{Lemma 2.6}).
\end{aligned}$$

The proof of claim (2) is done. For the proof of claim (1), we assume $x = z$ and use Lemma 3.1(1)(4). This completes the proof. $\square$

We are ready to prove Theorem 1.2.

Proof of Theorem 1.2. Let $M_{\boldsymbol{p}} = M_1^{p_n} M_3^{p'_n} M_2^{q_n} \cdots M_1^{p_1} M_3^{p'_1} M_2^{q_1}$ be the Perron-Frobenius matrix associated with $\boldsymbol{p} \in \mathcal{I}_n$. For a Perron-Frobenius eigenvector $\boldsymbol{v}$ of $M_{\boldsymbol{p}}$, we define positive vectors $\boldsymbol{x}^{(0)} := \boldsymbol{v}$ and $\boldsymbol{x}^{(i)} := M_1^{p_i} M_3^{p'_i} M_2^{q_i} \boldsymbol{x}^{(i-1)}$ for $i \in \{1, \dots, n\}$. Then $\boldsymbol{x}^{(n)} = M_{\boldsymbol{p}} \boldsymbol{v} = \lambda_{\boldsymbol{p}} \boldsymbol{v}$.

Suppose that $\boldsymbol{p}$ is asymmetric. By Corollaries 2.17 and 2.20, we can inductively prove that $\boldsymbol{x}^{(i)}|_1 \neq \boldsymbol{x}^{(i)}|_3$ for all $i \in \{0, \dots, n\}$. Proposition 3.2(2) tells us that

$$(\mathfrak{b}, \boldsymbol{x}^{(i-1)}) = (\delta_2^{q_i} \delta_1^{-p_i} \delta_3^{-p'_i} \circ \overset{\mathrm{l}}{\rightharpoonup}^{3q_i} \circ \overset{\mathrm{r}}{\rightharpoonup}^{p_i + p'_i})(\mathfrak{b}, \boldsymbol{x}^{(i)}) \quad \text{for } i \in \{1, \dots, n\}.$$

By the above equality for $i = 1, 2$, we obtain

$$\begin{aligned}
(\mathfrak{b}, \boldsymbol{v}) &= (\delta_2^{q_1} \delta_1^{-p_1} \delta_3^{-p'_1} \circ \overset{\mathrm{l}}{\rightharpoonup}^{3q_1} \circ \overset{\mathrm{r}}{\rightharpoonup}^{p_1 + p'_1})(\mathfrak{b}, \boldsymbol{x}^{(1)}) \\
&= (\delta_2^{q_1} \delta_1^{-p_1} \delta_3^{-p'_1} \circ \overset{\mathrm{l}}{\rightharpoonup}^{3q_1} \circ \overset{\mathrm{r}}{\rightharpoonup}^{p_1 + p'_1}) \circ (\delta_2^{q_2} \delta_1^{-p_2} \delta_3^{-p'_2} \circ \overset{\mathrm{l}}{\rightharpoonup}^{3q_2} \circ \overset{\mathrm{r}}{\rightharpoonup}^{p_2 + p'_2})(\mathfrak{b}, \boldsymbol{x}^{(2)}) \\
&= (\delta_2^{q_1} \delta_1^{-p_1} \delta_3^{-p'_1} \delta_2^{q_2} \delta_1^{-p_2} \delta_3^{-p'_2} \circ \overset{\mathrm{l}}{\rightharpoonup}^{3q_1} \circ \overset{\mathrm{r}}{\rightharpoonup}^{p_1 + p'_1} \circ \overset{\mathrm{l}}{\rightharpoonup}^{3q_2} \circ \overset{\mathrm{r}}{\rightharpoonup}^{p_2 + p'_2})(\mathfrak{b}, \boldsymbol{x}^{(2)}).
\end{aligned}$$

Repeating this argument, we finally obtain

$$(\mathfrak{b}, \boldsymbol{v}) = (\Phi_{\boldsymbol{p}}^{-1} \circ \overset{\mathrm{l}}{\rightharpoonup}^{3q_1} \circ \overset{\mathrm{r}}{\rightharpoonup}^{p_1 + p'_1} \circ \cdots \circ \overset{\mathrm{l}}{\rightharpoonup}^{3q_n} \circ \overset{\mathrm{r}}{\rightharpoonup}^{p_n + p'_n})(\mathfrak{b}, \lambda_{\boldsymbol{p}} \boldsymbol{v} = \boldsymbol{x}^{(n)}).$$

This means that

$$(\mathfrak{b}, \lambda_{\boldsymbol{p}} \boldsymbol{v}) \overset{\mathrm{r}}{\rightharpoonup}^{p_n + p'_n} \overset{\mathrm{l}}{\rightharpoonup}^{3q_n} \cdots \overset{\mathrm{r}}{\rightharpoonup}^{p_1 + p'_1} \overset{\mathrm{l}}{\rightharpoonup}^{3q_1} \Phi_{\boldsymbol{p}}(\mathfrak{b}, \boldsymbol{v}),$$

which is an Agol cycle of $\Phi_{\boldsymbol{p}}$ with length $\sum_{i=1}^n (p_i + p'_i + 3q_i)$.

Suppose that $\boldsymbol{p}$ is symmetric. By Corollary 2.17 $\boldsymbol{v}|_1 = \boldsymbol{v}|_3$ holds. A calculation shows that $\boldsymbol{x}^{(i)}|_1 = \boldsymbol{x}^{(i)}|_3$ for all $i \in \{0, \dots, n\}$. Applying Proposition 3.2(1), we have

$$(\mathfrak{b}, \boldsymbol{x}^{(i-1)}) = (\delta_2^{q_i} \delta_1^{-p_i} \delta_3^{-p_i} \circ \overset{\mathrm{l}}{\rightharpoonup}^{2q_i} \circ \overset{\mathrm{r}}{\rightharpoonup}^{p_i})(\mathfrak{b}, \boldsymbol{x}^{(i)}) \quad \text{for } i \in \{1, \dots, n\}. \tag{3.5}$$

Putting the above equalities (3.5) for each $i \in \{1, \cdots, n\}$ together, we can obtain

$$(\mathfrak{b}, \boldsymbol{v}) = (\Phi_{\boldsymbol{p}}^{-1} \circ \overset{\mathrm{l}}{\rightharpoonup}^{2q_1} \circ \overset{\mathrm{r}}{\rightharpoonup}^{p_1} \circ \cdots \circ \overset{\mathrm{l}}{\rightharpoonup}^{2q_n} \circ \overset{\mathrm{r}}{\rightharpoonup}^{p_n})(\mathfrak{b}, \lambda_{\boldsymbol{p}} \boldsymbol{v}).$$

This gives an Agol cycle of $\Phi_{\boldsymbol{p}}$ with length $\sum_{i=1}^n (p_i + 2q_i)$. We finished the proof. $\square$

Example 3.3. We present 2 examples for Agol cycles and their total splitting numbers. Recall that $\boldsymbol{v_p}$ is the normalized eigenvector with respect to $\lambda_{\boldsymbol{p}}$.

(1) For $\boldsymbol{p} = (1, 1, 1) \in \mathcal{I}_1$ symmetric, we have $\boldsymbol{v_p} = \begin{pmatrix} x \\ y \\ x \end{pmatrix}$ for some $x, y > 0$ and $M_{\boldsymbol{p}} \boldsymbol{v_p} = M_1 M_3 M_2 \boldsymbol{v_p} = \begin{pmatrix} 3x+y \\ 2x+y \\ 3x+y \end{pmatrix}$. Figure 11 illustrates an Agol cycle $(\mathfrak{b}, \lambda_{\boldsymbol{p}} \boldsymbol{v_p}) \overset{\mathrm{r}}{\rightharpoonup} \overset{\mathrm{l}}{\rightharpoonup}^2 \Phi_{\boldsymbol{p}}(\mathfrak{b}, \boldsymbol{v_p})$ of $\Phi_{\boldsymbol{p}} = \delta_1 \delta_3 \delta_2^{-1}$ with length 3. The splitting number of each maximal splitting in the Agol cycle is exactly 2. Hence, we have $N(\Phi_{\boldsymbol{p}}) = 2 \cdot 3 = 6$.

(2) For $\boldsymbol{p} = (1,2,1) \in \mathcal{I}_1$ asymmetric, $(\mathfrak{b}, \lambda_{\boldsymbol{p}}\boldsymbol{v}_{\boldsymbol{p}}) \overset{\mathrm{r}}{\rightharpoonup}{}^{3} \overset{\mathrm{l}}{\rightharpoonup}{}^{3} \Phi_{\boldsymbol{p}}(\mathfrak{b}, \boldsymbol{v}_{\boldsymbol{p}})$ is an Agol cycle of $\Phi_{\boldsymbol{p}} = \delta_1\delta_3^2\delta_2^{-1}$ with length 6 by Theorem 1.2. The splitting number of each maximal splitting in the Agol cycle is 1, except for the last maximal splitting $\overset{\mathrm{l}}{\rightharpoonup}$ with the splitting number 2. (See Figure 10(3)(4).) Hence, we have $N(\Phi_{\boldsymbol{p}}) = 7$.

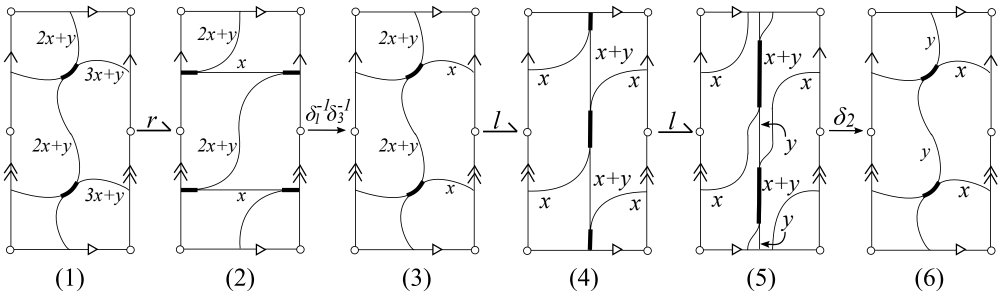

FIGURE 11. An Agol cycle of $\Phi_{\boldsymbol{p}}$ for $\boldsymbol{p} = (1,1,1)$. (1) $(\mathfrak{b}, M_1M_3M_2\boldsymbol{v}_{\boldsymbol{p}})$. (3) $(\mathfrak{b}, M_2\boldsymbol{v}_{\boldsymbol{p}})$. (6) $(\mathfrak{b}, \boldsymbol{v}_{\boldsymbol{p}})$.

Theorem 3.4. *For $\boldsymbol{p} = (p_n, p'_n, q_n, \ldots, p_1, p'_1, q_1) \in \mathcal{I}_n$ the total splitting number of an Agol cycle of $\Phi_{\boldsymbol{p}}$ is given by $N(\Phi_{\boldsymbol{p}}) = \sum_{i=1}^n (p_i + p'_i + 4q_i)$.*

Proof. By Proposition 3.2(2) in the case of asymmetric weights, i.e. $x \neq z$, we have a finite sequence $(\mathfrak{b}, M_1^pM_3^{p'}M_2^q\boldsymbol{x}) \overset{\mathrm{r}}{\rightharpoonup}{}^{p+p'} \overset{\mathrm{l}}{\rightharpoonup}{}^{3q} \delta_1^p\delta_3^{p'}\delta_2^{-q}(\mathfrak{b}, \boldsymbol{x})$. The total splitting number of the finite sequence (Definition 2.3(2)) is $p + p' + 4q$. The coefficient 4 of $4q$ comes from the total splitting number of a finite sequence $(\mathfrak{b}, M_2^q\boldsymbol{x}) \overset{\mathrm{l}}{\rightharpoonup}{}^{3} \delta_2^{-1}(\mathfrak{b}, M_2^{q-1}\boldsymbol{x})$ when $x \neq z$. See Figure 10. In the case of symmetric weights, i.e. $x = z$, Proposition 3.2(1) tells us that there exists a finite sequence $(\mathfrak{b}, M_1^pM_3^pM_2^q\boldsymbol{x}) \overset{\mathrm{r}}{\rightharpoonup}{}^{p} \overset{\mathrm{l}}{\rightharpoonup}{}^{2q} \delta_1^p\delta_3^p\delta_2^{-q}(\mathfrak{b}, \boldsymbol{x})$. Its total splitting number is $2(p + 2q) = p + p + 4q$ since the splitting number of a maximal splitting in this finite sequence is exactly 2.

The weight of $(\mathfrak{b}, M_{\boldsymbol{p}}\boldsymbol{v}_{\boldsymbol{p}})$ is given by $M_{\boldsymbol{p}}\boldsymbol{v}_{\boldsymbol{p}} = M_1^{p_n}M_3^{p'_n}M_2^{q_n} \cdots M_1^{p_1}M_3^{p'_1}M_2^{q_1}\boldsymbol{v}_{\boldsymbol{p}}$. By the repetition of the above argument, we can prove that $N(\Phi_{\boldsymbol{p}}) = \sum_{i=1}^n (p_i + p'_i + 4q_i)$. □

4. AGOL CYCLES OF PSEUDO-ANOSOV MAPS IN F_D

We introduce positive integers $S_i(\boldsymbol{p})$ and $A_i(\boldsymbol{p})$ for $\boldsymbol{p} \in \mathcal{I}_n$ as follows.

$$S_i(\boldsymbol{p}) = p_i + 2 \quad \text{and} \quad A_i(\boldsymbol{p}) = \begin{cases} 2p_i & \text{if } p'_i = 0, \\ 2p'_i & \text{if } p_i = 0, \\ p_i + p'_i + 2 & \text{otherwise.} \end{cases}$$

In this section, we prove the following result.

Theorem 4.1. *For $\boldsymbol{p} \in \mathcal{I}_n$ let $\phi_{\boldsymbol{p}} \in F_D$ be the pseudo-Anosov map and $M_{\boldsymbol{p}}$ be the Perron-Frobenius matrix associated with $\boldsymbol{p}$. Let $\boldsymbol{v} > \boldsymbol{0}$ be an eigenvector with respect to the Perron-Frobenius eigenvalue $\lambda_{\boldsymbol{p}}$ of $M_{\boldsymbol{p}}$. Then the Agol cycle length ℓ of $\phi_{\boldsymbol{p}}$ is*

$$\ell = \begin{cases} \sum_{i=1}^{n}(S_i(\boldsymbol{p}) + 2q_i) & \text{if } \boldsymbol{p} \text{ is symmetric,} \\ \sum_{i=1}^{n}(A_i(\boldsymbol{p}) + 3q_i) & \text{if } \boldsymbol{p} \text{ is asymmetric.} \end{cases}$$

Moreover, starting with the measured train track $(\mathfrak{b}_0, \mu_0) = (\mathfrak{b}_L, \lambda_{\boldsymbol{p}}\boldsymbol{v})$, a finite subsequence of the maximal splitting sequence

$$\begin{aligned} (\mathfrak{b}_0, \mu_0) \rightharpoondown^{S_n(\boldsymbol{p})+2q_n} \dots \rightharpoondown^{S_1(\boldsymbol{p})+2q_1} (\mathfrak{b}_\ell, \mu_\ell) \quad &\text{if } \boldsymbol{p} \text{ is symmetric,} \\ (\mathfrak{b}_0, \mu_0) \rightharpoondown^{A_n(\boldsymbol{p})+3q_n} \dots \rightharpoondown^{A_1(\boldsymbol{p})+3q_1} (\mathfrak{b}_\ell, \mu_\ell) \quad &\text{if } \boldsymbol{p} \text{ is asymmetric} \end{aligned}$$

forms an Agol cycle of $\phi_{\boldsymbol{p}}$. The consecutive maximal splittings consist of the following left, right and mixed maximal splittings

$$\begin{aligned} \rightharpoondown^{S_i(\boldsymbol{p})+2q_i} \quad &= \quad \overset{\mathrm{r}}{\rightharpoondown}\ \overset{\mathrm{l}}{\rightharpoondown}\ \overset{\mathrm{r}}{\rightharpoondown}^{p_i-1}\ \overset{\mathrm{l}}{\rightharpoondown}\ \overset{\mathrm{r}}{\rightharpoondown}\ \overset{\mathrm{l}}{\rightharpoondown}^{2q_i-1}, \\ \rightharpoondown^{A_i(\boldsymbol{p})+3q_i} \quad &= \quad \begin{cases} \overset{\mathrm{lr}}{\rightharpoondown}\ \overset{\mathrm{r}}{\rightharpoondown}^{2p_i-1}\ \overset{\mathrm{l}}{\rightharpoondown}^{3q_i} & \text{if } p'_i = 0, \\ \overset{\mathrm{lr}}{\rightharpoondown}\ \overset{\mathrm{r}}{\rightharpoondown}^{2p'_i-1}\ \overset{\mathrm{l}}{\rightharpoondown}^{3q_i} & \text{if } p_i = 0, \\ \overset{\mathrm{r}}{\rightharpoondown}\ \overset{\mathrm{l}}{\rightharpoondown}\ \overset{\mathrm{r}}{\rightharpoondown}^{p_i+p'_i-2}\ \overset{\mathrm{l}}{\rightharpoondown}^{2}\ \overset{\mathrm{r}}{\rightharpoondown}\ \overset{\mathrm{l}}{\rightharpoondown}^{3q_i-1} & \text{otherwise.} \end{cases} \end{aligned}$$

Figure 12(1) shows the measured train track $(\mathfrak{b}_L, \boldsymbol{x})$ that was defined in Section 1. Recall that the vector $\boldsymbol{x}$ reflects the weights of specific branches. Due to the switch condition, the weights on all remaining branches are determined. We introduce the measured train tracks $(\mathfrak{b}_R, \boldsymbol{x})$, $(\mathfrak{a}'_R, \boldsymbol{x})$ and $(\mathfrak{s}, \boldsymbol{x})$ in $\Sigma_{0,5}$ as in Figure 12(2), (4) and (5) respectively. Figure 12(3) gives the measured train track $\Delta(\mathfrak{a}'_R, \boldsymbol{x})$, where $\Delta = \sigma_1\sigma_2\sigma_3\sigma_1\sigma_2\sigma_1 \in \mathrm{MCG}(\Sigma_{0,5})$ is the π-rotation (Figure 12(6)).

For $\phi_{\boldsymbol{p}} = \sigma_1^{p_n}\sigma_3^{p'_n}\sigma_2^{-q_n} \dots \sigma_1^{p_1}\sigma_3^{p'_1}\sigma_2^{-q_1} \in F_D$ we call the product $\sigma_1^{p_j}\sigma_3^{p'_j}\sigma_2^{-q_j}$ the (j-th) block of $\phi_{\boldsymbol{p}}$ and say that the block is of type A (resp. A') if $p'_j = 0$ (resp. $p_j = 0$). Otherwise, we call it a type B block.

For the proof of Theorem 4.1 we consider each block $\sigma_1^{p_j}\sigma_3^{p'_j}\sigma_2^{-q_j}$ of $\phi_{\boldsymbol{p}}$. The transition matrix induced by $\sigma_1^{p_j}\sigma_3^{p'_j}\sigma_2^{-q_j}$ is $M_1^{p_j}M_3^{p'_j}M_2^{q_j}$. Depending on the type of the block, consecutive maximal splittings of $(\mathfrak{b}_L, M_1^{p_j}M_3^{p'_j}M_2^{q_j}\boldsymbol{x})$ will result in different finite sequences. Figure 13 is the central tool in this paper. It illustrates how finite sequences of maximal splittings transition one measured train track into another. The details are given in Lemmas 4.2, 4.4 and 4.5. We will see that the concatenation of suitable finite sequences gives an Agol cycle of the pseudo-Anosov map $\phi_{\boldsymbol{p}}$.

Lemma 4.2. *Let $q \in \mathbb{N}$ and $p, p' \in \mathbb{N}_0$. Let $\boldsymbol{x} = \begin{pmatrix} x \\ y \\ z \end{pmatrix} > \boldsymbol{0}$.*

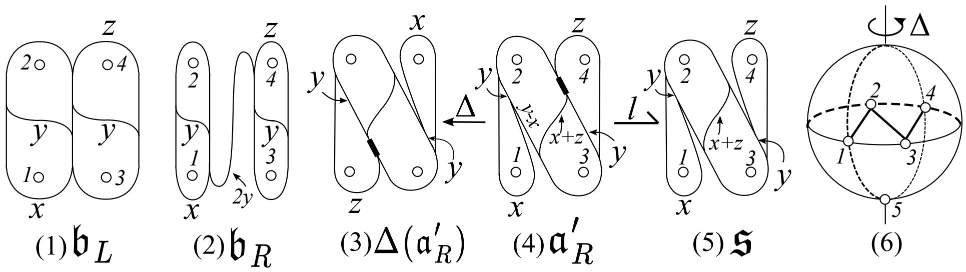

FIGURE 12. (1) $(\mathfrak{b}_L, \boldsymbol{x})$, (2) $(\mathfrak{b}_R, \boldsymbol{x})$, (3) $\Delta(\mathfrak{a}'_R, \boldsymbol{x})$, (4) $(\mathfrak{a}'_R, \boldsymbol{x})$, (5) $(\mathfrak{s}, \boldsymbol{x})$ for $\boldsymbol{x} = \left(\begin{smallmatrix} x \\ y \\ z \end{smallmatrix}\right)$. (6) $\Delta = \sigma_1\sigma_2\sigma_3\sigma_1\sigma_2\sigma_1 \in \mathrm{MCG}(\Sigma_{0,5})$. Figures (4)(5) illustrate a left maximal splitting $(\mathfrak{a}'_R, \boldsymbol{x}) \overset{\mathrm{l}}{\rightharpoondown} (\mathfrak{s}, \boldsymbol{x})$ for $z < y$.

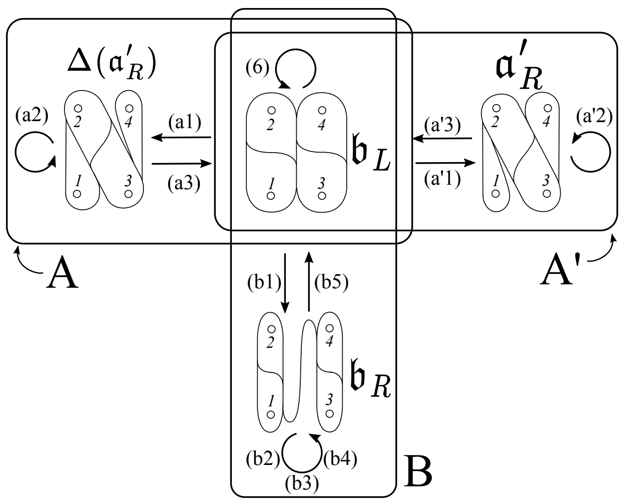

FIGURE 13. "Automaton" illustrating how the train tracks move between topological types under the operations in Lemmas 4.2, 4.4 and 4.5. Box B displays Lemma 4.2. Box A and A' display Lemmas 4.5 and 4.4 respectively.

(b1) *Suppose that* $p, p' > 0$. *Then*

$$(\mathfrak{b}_R, M_1^{p-1}M_3^{p'-1}M_2^q\boldsymbol{x}) = (\sigma_1^{-1}\sigma_3^{-1} \circ \overset{\mathrm{l}}{\rightharpoondown} \circ \overset{\mathrm{r}}{\rightharpoondown})(\mathfrak{b}_L, M_1^pM_3^{p'}M_2^q\boldsymbol{x}).$$

(b2) *Suppose that* $p > 0$. *Then*

$$(\mathfrak{b}_R, M_1^{p-1}M_3^{p-1}M_2^q\boldsymbol{x}) = \begin{cases} (\sigma_1^{-1}\sigma_3^{-1} \circ \overset{\mathrm{r}}{\rightharpoondown})(\mathfrak{b}_R, M_1^pM_3^pM_2^q\boldsymbol{x}) & \textit{if } x = z, \\ (\sigma_1^{-1}\sigma_3^{-1} \circ \overset{\mathrm{r}}{\rightharpoondown}^2)(\mathfrak{b}_R, M_1^pM_3^pM_2^q\boldsymbol{x}) & \textit{if } x \neq z. \end{cases}$$

(b3) *Suppose that* $p > p' \geq 0$. *Then*

$$(\mathfrak{b}_R, M_1^{p-1}M_3^{p'}M_2^q\boldsymbol{x}) = (\sigma_1^{-1} \circ \overset{\mathrm{r}}{\rightharpoondown})(\mathfrak{b}_R, M_1^pM_3^{p'}M_2^q\boldsymbol{x}).$$

(b4) *Suppose that* $0 \le p < p'$. *Then*

$$(\mathfrak{b}_R, M_1^p M_3^{p'-1} M_2^q \boldsymbol{x}) = (\sigma_3^{-1} \circ \overset{\mathrm{r}}{\rightharpoonup})(\mathfrak{b}_R, M_1^p M_3^{p'} M_2^q \boldsymbol{x}).$$

(b5) $(\mathfrak{b}_L, M_2^{q-1}\boldsymbol{x}) = \begin{cases} (\sigma_2 \circ \overset{\mathrm{l}}{\rightharpoonup} \circ \overset{\mathrm{r}}{\rightharpoonup} \circ \overset{\mathrm{l}}{\rightharpoonup})(\mathfrak{b}_R, M_2^q \boldsymbol{x}) & \text{if } x = z, \\ (\sigma_2 \circ \overset{\mathrm{l}}{\rightharpoonup}{}^2 \circ \overset{\mathrm{r}}{\rightharpoonup} \circ \overset{\mathrm{l}}{\rightharpoonup}{}^2)(\mathfrak{b}_R, M_2^q \boldsymbol{x}) & \text{if } x \neq z. \end{cases}$

(6) $(\mathfrak{b}_L, M_2^{q-1}\boldsymbol{x}) = \begin{cases} (\sigma_2 \circ \overset{\mathrm{l}}{\rightharpoonup}{}^2)(\mathfrak{b}_L, M_2^q \boldsymbol{x}) & \text{if } x = z, \\ (\sigma_2 \circ \overset{\mathrm{l}}{\rightharpoonup}{}^3)(\mathfrak{b}_L, M_2^q \boldsymbol{x}) & \text{if } x \neq z. \end{cases}$

Proof. Figure 14 shows that $(\mathfrak{b}_L, M_1 M_3 \boldsymbol{a} = \begin{pmatrix} a+b \\ b \\ b+c \end{pmatrix}) \overset{\mathrm{r}}{\rightharpoonup} \overset{\mathrm{l}}{\rightharpoonup} \sigma_1\sigma_3(\mathfrak{b}_R, \boldsymbol{a})$ for $\boldsymbol{a} = \begin{pmatrix} a \\ b \\ c \end{pmatrix} > \boldsymbol{0}$. In other words, $(\mathfrak{b}_R, \boldsymbol{a}) = (\sigma_1^{-1}\sigma_3^{-1} \circ \overset{\mathrm{l}}{\rightharpoonup} \circ \overset{\mathrm{r}}{\rightharpoonup})(\mathfrak{b}_L, M_1 M_3 \boldsymbol{a})$. Choosing $\boldsymbol{a} = M_1^{p-1} M_3^{p'-1} M_2^q \boldsymbol{x}$ as a positive vector, we obtain claim (b1).

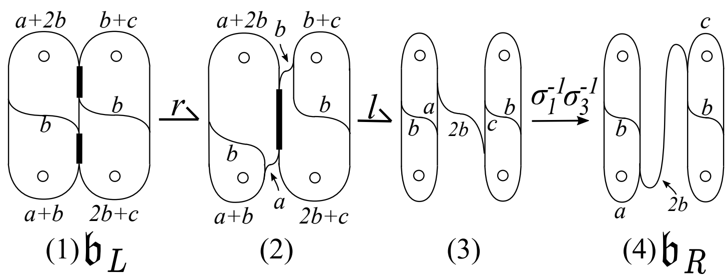

FIGURE 14. Proof of Lemma 4.2(b1). (1) $(\mathfrak{b}_L, M_1 M_3 \boldsymbol{a})$. (4) $(\mathfrak{b}_R, \boldsymbol{a})$.

It is enough to prove the remaining claims when $q = 1$. For claim (b2), we set $(\mathfrak{b}_0, \mu_0) = (\mathfrak{b}_R, M_1^p M_3^p M_2 \boldsymbol{x})$. The proof is similar to that of Lemma 3.1(1). Figure 15 illustrates the proof of (b2) when $x < z$. In the case $x = z$, the two large branches of $(\mathfrak{b}_R, M_1^p M_3^p M_2 \boldsymbol{x})$ have the same weight. (c.f. Figure 15(1).) Applying a maximal splitting, we obtain the right maximal splitting $(\mathfrak{b}_R, M_1^p M_3^p M_2 \boldsymbol{x}) \overset{\mathrm{r}}{\rightharpoonup} \sigma_1\sigma_3(\mathfrak{b}_R, M_1^{p-1} M_3^{p-1} M_2 \boldsymbol{x})$. This completes the proof of claim (b2).

The proof of claim (b3) (resp. (b4)) is similar to that of Lemma 3.1(2) (resp. Lemma 3.1(3)) and we omit the proof.

Before proving claim (b5), we first prove claim (6). We consider the measured train track $(\mathfrak{b}_0, \mu_0) = (\mathfrak{b}_L, M_2 \boldsymbol{x} = \begin{pmatrix} x \\ x+y+z \\ z \end{pmatrix})$ when $x \neq z$. We may suppose that $x < z$. Applying 3 maximal splittings (see Figure 16(1)–(4)), we have 3 left maximal splittings

$$(\mathfrak{b}_0, \mu_0) = (\mathfrak{b}_L, M_2 \boldsymbol{x}) \overset{\mathrm{l}}{\rightharpoonup} (\mathfrak{b}_1, \mu_1) = (\mathfrak{s}, M_2 \boldsymbol{x}) \overset{\mathrm{l}}{\rightharpoonup} (\mathfrak{b}_2, \mu_2) \overset{\mathrm{l}}{\rightharpoonup} (\mathfrak{b}_3, \mu_3) = \sigma_2^{-1}(\mathfrak{b}_L, \boldsymbol{x}). \tag{4.1}$$

This gives claim (6) when $x < z$.

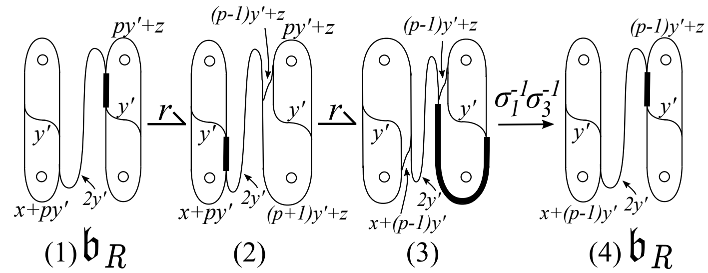

FIGURE 15. Proof of Lemma 4.2(b2) when $x < z$. (1) $(\mathfrak{b}_R, M_1^p M_3^p M_2\boldsymbol{x})$. (4) $(\mathfrak{b}_R, M_1^{p-1}M_3^{p-1}M_2\boldsymbol{x})$.

We turn to the case $x = z$. Applying 2 maximal splittings, we obtain 2 left maximal splittings

$$(\mathfrak{b}_0, \mu_0) = (\mathfrak{b}_L, M_2\boldsymbol{x})\overset{\mathrm{l}}{\rightharpoonup}(\mathfrak{b}_1, \mu_1) = (\mathfrak{s}, M_2\boldsymbol{x})\overset{\mathrm{l}}{\rightharpoonup}(\mathfrak{b}_2, \mu_2) = \sigma_2^{-1}(\mathfrak{b}_L, \boldsymbol{x}).$$

This gives the proof of claim (6) when $x = z$.

We finally prove claim (b5). Consider the measured train track $(\mathfrak{b}_0, \mu_0) = (\mathfrak{b}_R, M_2\boldsymbol{x})$ when $x \neq z$. We may suppose that $x < z$. Figures 16(1')–(3') and (2) show that $(\mathfrak{b}_0, \mu_0) = (\mathfrak{b}_R, M_2\boldsymbol{x})\overset{\mathrm{l}}{\rightharpoonup}^2\overset{\mathrm{r}}{\rightharpoonup}(\mathfrak{s}, M_2\boldsymbol{x})$. Taking the last two maximal splittings from the finite sequence (4.1), we have $(\mathfrak{s}, M_2\boldsymbol{x})\overset{\mathrm{l}}{\rightharpoonup}^2\sigma_2^{-1}(\mathfrak{b}_L, \boldsymbol{x})$. Putting them together, we have

$$(\mathfrak{b}_0, \mu_0) = (\mathfrak{b}_R, M_2\boldsymbol{x})\overset{\mathrm{l}}{\rightharpoonup}^2\overset{\mathrm{r}}{\rightharpoonup}(\mathfrak{s}, M_2\boldsymbol{x})\overset{\mathrm{l}}{\rightharpoonup}^2\sigma_2^{-1}(\mathfrak{b}_L, \boldsymbol{x}).$$

This gives claim (b5) when $x < z$.

In the case $x = z$, the measured train track $(\mathfrak{b}_R, M_2\boldsymbol{x})$ has two large branches with maximal weight. This gives the finite sequence $(\mathfrak{b}_L, M_2\boldsymbol{x})\overset{\mathrm{l}}{\rightharpoonup}\overset{\mathrm{r}}{\rightharpoonup}(\mathfrak{s}, M_2\boldsymbol{x})\overset{\mathrm{l}}{\rightharpoonup}\sigma_2^{-1}(\mathfrak{b}_L, \boldsymbol{x})$. This completes the proof. □

Let $(\mathfrak{b}_L, M_1^pM_3^pM_2^q\boldsymbol{x})$ be a measured train track, where the measure $M_1^pM_3^pM_2^q\boldsymbol{x}$ is preceded by a type B block. By repeatedly applying the last lemma, we now compute the maximal splittings of $(\mathfrak{b}_L, M_1^pM_3^pM_2^q\boldsymbol{x})$.

Proposition 4.3 (Type B block)**.** *Let $p, p', q \in \mathbb{N}$. Let $\boldsymbol{x} = \begin{pmatrix} x \\ y \\ z \end{pmatrix} > \mathbf{0}$.*

(1) *(Symmetric case.)* $(\mathfrak{b}_L, \boldsymbol{x}) = (\sigma_2^q\sigma_1^{-p}\sigma_3^{-p}\circ \rightharpoonup^{p+2+2q})(\mathfrak{b}_L, M_1^pM_3^pM_2^q\boldsymbol{x})$ *if $x = z$. The consecutive maximal splittings consist of the following left and right maximal splittings*

$$\rightharpoonup^{p+2+2q} = \overset{\mathrm{l}}{\rightharpoonup}^{2q-1}\circ\overset{\mathrm{r}}{\rightharpoonup}\circ\overset{\mathrm{l}}{\rightharpoonup}\circ\overset{\mathrm{r}}{\rightharpoonup}^{p-1}\circ\overset{\mathrm{l}}{\rightharpoonup}\circ\overset{\mathrm{r}}{\rightharpoonup}.$$

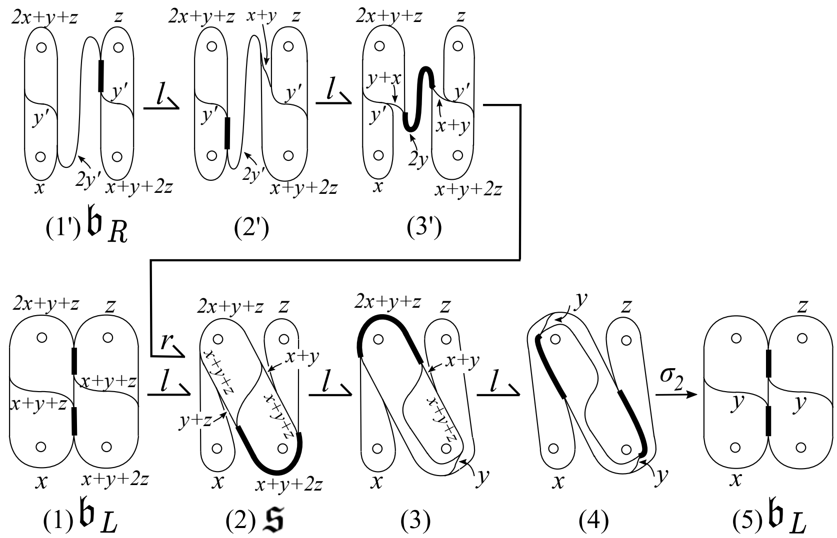

FIGURE 16. (1)–(5) Proof of Lemma 4.2(6) when $x < z$. (1')–(3')(2)–(5) Proof of Lemma 4.2(b5) when $x < z$.

(2) *(Asymmetric case.)* $(\mathfrak{b}_L, \boldsymbol{x}) = (\sigma_2^q\sigma_1^{-p}\sigma_3^{-p'} \circ \rightharpoonup^{p+p'+2+3q})(\mathfrak{b}_L, M_1^pM_3^{p'}M_2^q\boldsymbol{x})$ *if* $x \neq z$, *possibly* $p = p'$. *The consecutive maximal splittings consist of the following left and right maximal splittings*

$$\rightharpoonup^{p+p'+2+3q} = \overset{\mathrm{l}}{\rightharpoonup}^{3q-1} \circ \overset{\mathrm{r}}{\rightharpoonup} \circ \overset{\mathrm{l}}{\rightharpoonup}^{2} \circ \overset{\mathrm{r}}{\rightharpoonup}^{p+p'-2} \circ \overset{\mathrm{l}}{\rightharpoonup} \circ \overset{\mathrm{r}}{\rightharpoonup}.$$

Proof. We prove claim (2). Suppose that $x \neq z$. We may assume that $p < p'$. (The proof for the case $p \geq p'$ can be treated in the same manner.) We have

$$\begin{aligned}
(\mathfrak{b}_R, M_1^{p-1}M_3^{p'-1}M_2^q\boldsymbol{x}) &= (\sigma_1^{-1}\sigma_3^{-1} \circ \overset{\mathrm{l}}{\rightharpoonup} \circ \overset{\mathrm{r}}{\rightharpoonup})(\mathfrak{b}_L, M_1^pM_3^{p'}M_2^q\boldsymbol{x}) \ \text{(Lemma 4.2(b1))},\\
(\mathfrak{b}_R, M_1^{p-1}M_3^{p-1}M_2^q\boldsymbol{x}) &= (\sigma_3^{-(p'-p)} \circ \overset{\mathrm{r}}{\rightharpoonup}^{p'-p})(\mathfrak{b}_R, M_1^{p-1}M_3^{p'-1}M_2^q\boldsymbol{x}) \ \text{(Lemma 4.2(b4))},\\
(\mathfrak{b}_R, M_2^q\boldsymbol{x}) &= ((\sigma_1\sigma_3)^{-(p-1)} \circ \overset{\mathrm{r}}{\rightharpoonup}^{2p-2})(\mathfrak{b}_R, M_1^{p-1}M_3^{p-1}M_2^q\boldsymbol{x}) \ \text{(Lemma 4.2(b2))},\\
(\mathfrak{b}_L, \boldsymbol{x}) &= (\sigma_2^q \circ \overset{\mathrm{l}}{\rightharpoonup}^{3(q-1)} \circ \overset{\mathrm{l}}{\rightharpoonup}^{2} \circ \overset{\mathrm{r}}{\rightharpoonup} \circ \overset{\mathrm{l}}{\rightharpoonup}^{2})(\mathfrak{b}_R, M_2^q\boldsymbol{x}) \ \text{(Lemma 4.2(b5),(6))}.
\end{aligned}$$

By the above equalities together with Lemma 2.6, we obtain

$$(\mathfrak{b}_L, \boldsymbol{x}) = (\sigma_2^q\sigma_1^{-p}\sigma_3^{-p'} \circ \overset{\mathrm{l}}{\rightharpoonup}^{3q-1} \circ \overset{\mathrm{r}}{\rightharpoonup} \circ \overset{\mathrm{l}}{\rightharpoonup}^{2} \circ \overset{\mathrm{r}}{\rightharpoonup}^{p+p'-2} \circ \overset{\mathrm{l}}{\rightharpoonup} \circ \overset{\mathrm{r}}{\rightharpoonup})(\mathfrak{b}_L, M_1^pM_3^{p'}M_2^q\boldsymbol{x}).$$

This completes the proof of (2). The proof of claim (1) is left to the reader. □

Lemma 4.4. *Let* $q, s \in \mathbb{N}$. *Let* $\boldsymbol{x} = \begin{pmatrix} x \\ y \\ z \end{pmatrix} > \mathbf{0}$.

(a'1) $(\mathfrak{a}'_R, M_3^{s-1}M_2^q\boldsymbol{x}) = (\sigma_3^{-1} \circ \overset{\mathrm{r}}{\rightharpoonup} \circ \overset{\mathrm{lr}}{\rightharpoonup})(\mathfrak{b}_L, M_3^sM_2^q\boldsymbol{x})$.

(a'2) $(\mathfrak{a}'_R, M_3^{s-1}M_2^q\boldsymbol{x}) = (\sigma_3^{-1}\circ \overset{\mathrm{r}}{\rightharpoonup}{}^2)(\mathfrak{a}'_R, M_3^sM_2^q\boldsymbol{x})$.

(a'3) $(\mathfrak{b}_L, M_2^{q-1}\boldsymbol{x}) = (\sigma_2\circ \overset{1}{\rightharpoonup}{}^3)(\mathfrak{a}'_R, M_2^q\boldsymbol{x})$ *if* $x\neq z$.

Proof. It is sufficient to prove the lemma when $q=1$. Consider the maximal splitting starting from $(\mathfrak{b}_L, M_3^sM_2\boldsymbol{x} = \begin{pmatrix} x \\ y' \\ sy'+z\end{pmatrix})$, where $y' = x+y+z$. Figure 17 shows that

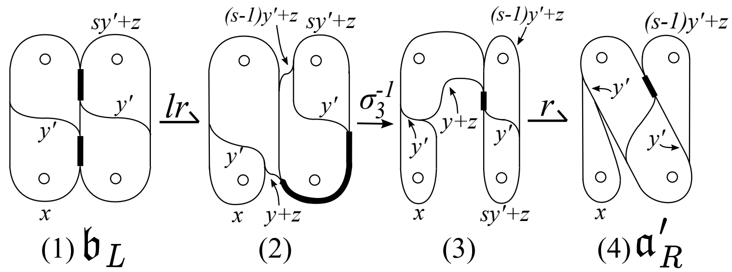

FIGURE 17. Proof of Lemma 4.4(a'1). (1) $(\mathfrak{b}_L, M_3^sM_2\boldsymbol{x})$. (4) $(\mathfrak{a}'_R, M_3^{s-1}M_2\boldsymbol{x})$.

$$(\mathfrak{a}'_R, M_3^{s-1}M_2\boldsymbol{x}) = (\overset{\mathrm{r}}{\rightharpoonup}\circ\sigma_3^{-1}\circ\overset{\mathrm{lr}}{\rightharpoonup})(\mathfrak{b}_L, M_3^sM_2\boldsymbol{x}) = (\sigma_3^{-1}\circ\overset{\mathrm{r}}{\rightharpoonup}\circ\overset{\mathrm{lr}}{\rightharpoonup})(\mathfrak{b}_L, M_3^sM_2\boldsymbol{x}).$$

The proof of claim (a'1) is done. For the proof of claim (a'2), see Figure 18.

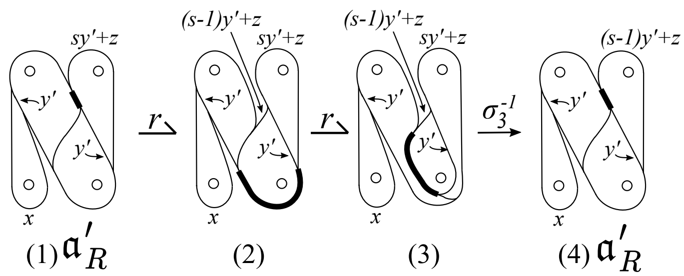

FIGURE 18. Proof of Lemma 4.4(a'2). (1) $(\mathfrak{a}'_R, M_3^sM_2\boldsymbol{x} = \begin{pmatrix} x \\ y' \\ sy'+z\end{pmatrix})$, where $y' = x+y+z$. (4) $(\mathfrak{a}'_R, M_3^{s-1}M_2\boldsymbol{x})$.

We prove claim (a'3). Consider the measured train track $(\mathfrak{a}'_R, M_2\boldsymbol{x})$. We may suppose that $x<z$. Applying 3 maximal splittings consecutively, we obtain 3 left maximal splittings $(\mathfrak{a}'_R, M_2\boldsymbol{x})\overset{1}{\rightharpoonup}(\mathfrak{s}, M_2\boldsymbol{x})\overset{1}{\rightharpoonup}{}^2\sigma_2^{-1}(\mathfrak{b}_L, \boldsymbol{x})$. See Figure 19. We finished the proof. □

Recall that $\Delta = \sigma_1\sigma_2\sigma_3\sigma_1\sigma_2\sigma_1$ is the π-rotation (Figure 12(6)).

Lemma 4.5. *Let* $q, s\in\mathbb{N}$. *Let* $\boldsymbol{x} = \begin{pmatrix} x \\ y \\ z\end{pmatrix} > \boldsymbol{0}$ *and* $J = \begin{pmatrix} 0&0&1 \\ 0&1&0 \\ 1&0&0\end{pmatrix}$.

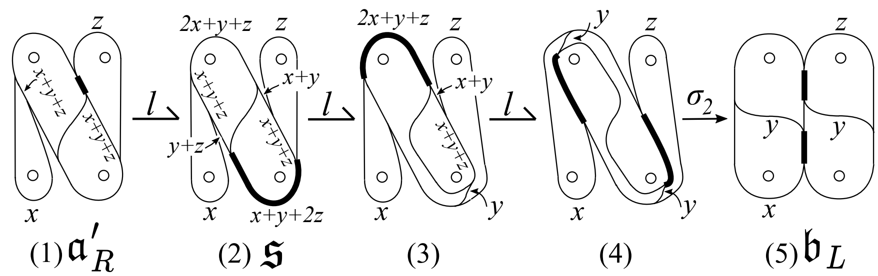

FIGURE 19. Proof of Lemma 4.4(a'3). (1) $(\mathfrak{a}'_R, M_2\boldsymbol{x})$. (2) $(\mathfrak{s}, M_2\boldsymbol{x})$. (4) $(\mathfrak{b}_L, \boldsymbol{x})$.

(a1) $\Delta(\mathfrak{a}'_R, M_3^{s-1}M_2^q J\boldsymbol{x}) = (\sigma_1^{-1} \circ \overset{\mathrm{r}}{\rightharpoonup} \circ \overset{\mathrm{lr}}{\rightharpoonup})(\mathfrak{b}_L, M_1^s M_2^q \boldsymbol{x})$.
(a2) $\Delta(\mathfrak{a}'_R, M_3^{s-1}M_2^q J\boldsymbol{x}) = (\sigma_1^{-1} \circ \overset{\mathrm{r}}{\rightharpoonup}{}^2 \circ \Delta)(\mathfrak{a}'_R, M_3^s M_2^q J\boldsymbol{x})$.
(a3) $(\mathfrak{b}_L, M_2^{q-1}\boldsymbol{x}) = (\sigma_2 \circ \overset{\mathrm{l}}{\rightharpoonup}{}^3 \circ \Delta)(\mathfrak{a}'_R, M_2^q J\boldsymbol{x})$ *if* $x \neq z$.

Proof. Observe that $\Delta(\mathfrak{b}_L, M_3^s M_2^q J\boldsymbol{x}) = (\mathfrak{b}_L, M_1^s M_2^q \boldsymbol{x})$. By $\Delta\sigma_i^{\pm 1} = \sigma_j^{\pm 1}\Delta$ for the pair $(i, j) = (1, 3)$ or $(3, 1)$, the proof is analogous to that of Lemma 4.4. □

Let $(\mathfrak{b}_L, M_1^s M_2^q \boldsymbol{x})$ or $(\mathfrak{b}_L, M_3^s M_2^q \boldsymbol{x})$ be a measured train track, where the measures are preceded by a type A and A' block respectively. We now compute the maximal splittings of the measured train tracks.

Proposition 4.6 (Type A/A' block for (1)/(2))**.** *Let* $q, s \in \mathbb{N}$. *Let* $\boldsymbol{x} = \left(\begin{smallmatrix} x \\ y \\ z \end{smallmatrix}\right) > \boldsymbol{0}$.

(1) $(\mathfrak{b}_L, \boldsymbol{x}) = (\sigma_2^q \sigma_1^{-s} \circ \overset{\mathrm{l}}{\rightharpoonup}{}^{3q} \circ \overset{\mathrm{r}}{\rightharpoonup}{}^{2s-1} \circ \overset{\mathrm{lr}}{\rightharpoonup})(\mathfrak{b}_L, M_1^s M_2^q \boldsymbol{x})$.
(2) $(\mathfrak{b}_L, \boldsymbol{x}) = (\sigma_2^q \sigma_3^{-s} \circ \overset{\mathrm{l}}{\rightharpoonup}{}^{3q} \circ \overset{\mathrm{r}}{\rightharpoonup}{}^{2s-1} \circ \overset{\mathrm{lr}}{\rightharpoonup})(\mathfrak{b}_L, M_3^s M_2^q \boldsymbol{x})$.

Proof. By a similar argument as in the proof of Proposition 4.3, one can prove claims (1) and (2). In the case of Proposition 4.3, we used Lemma 4.2. For the proof of (1) (resp. (2)), we use Lemma 4.5 (resp. Lemma 4.4) together with Lemma 4.2(6). □

Proof of Theorem 4.1. As in the proof of Theorem 1.2, for a Perron-Frobenius eigenvector $\boldsymbol{v}$ of $M_{\boldsymbol{p}}$ we define positive vectors $\boldsymbol{x}^{(0)} := \boldsymbol{v}$ and $\boldsymbol{x}^{(i)} := M_1^{p_i} M_3^{p'_i} M_2^{q_i} \boldsymbol{x}^{(i-1)}$ for $i \in \{1, \ldots, n\}$. Suppose that $\boldsymbol{p}$ is asymmetric. By Propositions 4.3(2) and 4.6, we have

$$(\mathfrak{b}_L, \boldsymbol{x}^{(i-1)}) = (\sigma_2^{q_i} \sigma_1^{-p_i} \sigma_3^{-p'_i} \circ \rightharpoonup^{A_i + 3q_i})(\mathfrak{b}_L, \boldsymbol{x}^{(i)}) \text{ for } i \in \{1, \ldots, n\},$$

where $A_i = A_i(\boldsymbol{p})$ is the positive integer defined in Section 1. This gives us

$$(\mathfrak{b}_L, \boldsymbol{v} = \boldsymbol{x}^{(0)}) = (\phi_{\boldsymbol{p}}^{-1} \circ \rightharpoonup^{A_1 + 3q_1} \circ \cdots \circ \rightharpoonup^{A_n + 3q_n})(\mathfrak{b}_L, \lambda_{\boldsymbol{p}} \boldsymbol{v} = \boldsymbol{x}^{(n)}).$$

This means that

$$(\mathfrak{b}_0, \mu_0) = (\mathfrak{b}_L, \lambda_{\boldsymbol{p}} \boldsymbol{v}) \rightharpoonup^{A_n + 3q_n} \cdots \rightharpoonup^{A_1 + 3q_1} \phi_{\boldsymbol{p}}(\mathfrak{b}_L, \boldsymbol{v}) = (\mathfrak{b}_\ell, \mu_\ell)$$

is an Agol cycle of $\phi_{\boldsymbol{p}}$ with length ℓ. The consecutive $A_i + 3q_i$ maximal splittings $\rightharpoonup^{A_i+3q_i}$ are given by Proposition 4.3(2) when the i-th block of $\phi_{\boldsymbol{p}}$ is of type B. The maximal splittings are given by Propositions 4.6 when the i-th block is of type A or A'.

The proof of the theorem when $\boldsymbol{p}$ is symmetric is left to the reader. $\square$

Example 4.7. We present 2 examples for Agol cycles and their total splitting numbers.

(1) For $\boldsymbol{p} = (1, 2, 1) \in \mathcal{I}_1$ asymmetric, an Agol cycle of $\phi_{\boldsymbol{p}}$ is given by

$$(\mathfrak{b}_L, \lambda_{\boldsymbol{p}}\boldsymbol{v}_{\boldsymbol{p}}) \overset{\mathrm{r}}{\rightharpoonup} \overset{\mathrm{l}}{\rightharpoonup} \overset{\mathrm{r}}{\rightharpoonup} \overset{\mathrm{l}}{\rightharpoonup}^{2} \overset{\mathrm{r}}{\rightharpoonup} \overset{\mathrm{l}}{\rightharpoonup}^{2} \phi_{\boldsymbol{p}}(\mathfrak{b}_L, \boldsymbol{v}_{\boldsymbol{p}})$$

whose length is 8. The splitting number of each maximal splitting is 1, except for the first maximal splitting $\overset{\mathrm{r}}{\rightharpoonup}$ whose splitting number is 2 (Figure 14(1)(2)). Hence, we have $N(\phi_{\boldsymbol{p}}) = 9$.

(2) For $\boldsymbol{p} = (1, 0, 1, 0, 1, 1) \in \mathcal{I}_2$ asymmetric, an Agol cycle of $\phi_{\boldsymbol{p}}$ is given by

$$(\mathfrak{b}_L, \lambda_{\boldsymbol{p}}\boldsymbol{v}_{\boldsymbol{p}}) \overset{\mathrm{lr}}{\rightharpoonup} \overset{\mathrm{r}}{\rightharpoonup} \overset{\mathrm{l}}{\rightharpoonup}^{3} \overset{\mathrm{lr}}{\rightharpoonup} \overset{\mathrm{r}}{\rightharpoonup} \overset{\mathrm{l}}{\rightharpoonup}^{3} \phi_{\boldsymbol{p}}(\mathfrak{b}_L, \boldsymbol{v}_{\boldsymbol{p}}),$$

whose length is 10. The splitting number of each maximal splitting is 1, except for the 2 mixed maximal splittings $\overset{\mathrm{lr}}{\rightharpoonup}$, whose splitting number is 2 (Figure 17(1)(2)). Hence, we have $N(\phi_{\boldsymbol{p}}) = 12$.

Theorem 4.8. *For $\boldsymbol{p} \in \mathcal{I}_n$ the total splitting number of an Agol cycle of $\phi_{\boldsymbol{p}}$ is given by We have $N(\phi_{\boldsymbol{p}}) = \sum_{i=1}^{n}(A_i(\boldsymbol{p}) + 4q_i)$.*

Proof. For each finite sequence of maximal splittings given by Propositions 4.3 and 4.6, we compute its total splitting number. For instance, take a finite sequence

$$(\mathfrak{b}_L, M_1^{p_i} M_2^{q_i}\boldsymbol{x}) \overset{\mathrm{lr}}{\rightharpoonup} \overset{\mathrm{r}}{\rightharpoonup}^{2p_i - 1} \overset{\mathrm{l}}{\rightharpoonup}^{3q_i} \sigma_1^{p_i}\sigma_2^{-q_i}(\mathfrak{b}_L, \boldsymbol{x})$$

given by Proposition 4.6(1). Counting the large branches with maximal weight in each maximal splitting, one sees that its total splitting number is $2p_i + 4q_i (= A_i(\boldsymbol{p}) + 4q_i)$. One can prove the total splitting number of the Agol cycle for $\phi_{\boldsymbol{p}}$ given by Theorem 4.1 equals the sum of $A_i(\boldsymbol{p}) + 4q_i$ over i, that is $\sum_{i=1}^{n}(A_i(\boldsymbol{p}) + 4q_i)$. $\square$

Proof of Theorem 1.3. Theorems 3.4 and 4.8 immediately give the desired statement. $\square$

5. Conjugacy classes of pseudo-Anosov maps in F_T and F_D

In the final section we classify conjugacy classes of pseudo-Anosov maps in the semigroups F_T and F_D. To do this, we define maps $T : \mathbb{N}_0^{3n} \to \mathbb{N}_0^{3n}$, called the *shift*, and $f : \mathbb{N}_0^{3n} \to \mathbb{N}_0^{3n}$, called the *flip*, as follows. For $\boldsymbol{p} = (p_n, p'_n, q_n, \ldots, p_1, p'_1, q_1) \in \mathbb{N}_0^{3n}$

$$\begin{aligned} T(\boldsymbol{p}) &= (p_{n-1}, p'_{n-1}, q_{n-1}, \ldots, p_1, p'_1, q_1, p_n, p'_n, q_n), \\ f(\boldsymbol{p}) &= (p'_n, p_n, q_n, \ldots, p'_1, p_1, q_1). \end{aligned}$$

The shift T permutes by three entries and the flip f interchanges p_i and p'_i for all $i \in \{1, \dots, n\}$. Note that $\boldsymbol{p}$ is symmetric if and only if the flip f preserves $\boldsymbol{p}$, i.e. $f(\boldsymbol{p}) = \boldsymbol{p}$. Let $\boldsymbol{p} \in \mathcal{I}_n$ and $\boldsymbol{t} \in \mathcal{I}_m$. We write $\boldsymbol{p} \sim \boldsymbol{t}$ if $n = m$ and $T^k(\boldsymbol{p}) \in \{\boldsymbol{t}, f(\boldsymbol{t})\}$ for some $k \geq 0$.

Theorem 5.1. *Let $\boldsymbol{p} \in \mathcal{I}_n$ and $\boldsymbol{t} \in \mathcal{I}_m$. The following are equivalent.*

(1) $\boldsymbol{p} \sim \boldsymbol{t}$.
(2) $\Phi_{\boldsymbol{p}}$ *and* $\Phi_{\boldsymbol{t}}$ *are conjugate in* $\mathrm{MCG}(\Sigma_{1,2})$.
(3) $\phi_{\boldsymbol{p}}$ *and* $\phi_{\boldsymbol{t}}$ *are conjugate in* $\mathrm{MCG}(\Sigma_{0,5})$.

Proof. Suppose that $\boldsymbol{p} \sim \boldsymbol{t}$. This means that $T^k(\boldsymbol{p}) = \boldsymbol{t}$ or $T^k(\boldsymbol{p}) = f(\boldsymbol{t})$ for some $k \geq 0$. By the definition of the shift T, $\Phi_{\boldsymbol{p}}$ and $\Phi_{T(\boldsymbol{p})}$ (resp. $\phi_{\boldsymbol{p}}$ and $\phi_{T(\boldsymbol{p})}$) are conjugate. Note that $\Phi_{\boldsymbol{p}}$ and $\Phi_{f(\boldsymbol{p})}$ (resp. $\phi_{\boldsymbol{p}}$ and $\phi_{f(\boldsymbol{p})}$) are also conjugate. In this case, a conjugacy is given by F (resp. Δ), where $F : \Sigma_{1,2} \to \Sigma_{1,2}$ is the π-rotation along the simple closed curve c_2 (Figure 2(1)).

Thus the condition (1) implies the conditions (2) and (3).

To see the that (2) implies (1), suppose that $\Phi_{\boldsymbol{p}}$ and $\Phi_{\boldsymbol{t}}$ are conjugate in $\mathrm{MCG}(\Sigma_{1,2})$. By Theorem 2.5 their periodic splitting sequences are combinatorially isomorphic and their Agol cycle lengths are equal. Notice that by Theorem 1.2 $\boldsymbol{p}$ is symmetric if and only if $\boldsymbol{t}$ is symmetric. We now prove that $\boldsymbol{p} \sim \boldsymbol{t}$ when both $\boldsymbol{p}$ and $\boldsymbol{t}$ are asymmetric. (The proof for the symmetric case is analogous.) Let ℓ be the Agol cycle lengths of $\Phi_{\boldsymbol{p}}$ and $\Phi_{\boldsymbol{t}}$. For $\boldsymbol{p} = (p_n, p'_n, q_n, \dots, p_1, p'_1, q_1) \in \mathcal{I}_n$ and $\boldsymbol{t} = (t_m, t'_m, u_m, \dots, t_1, t'_1, u_1) \in \mathcal{I}_m$, Theorem 1.2 tells us that

$$(\mathfrak{b}, \lambda_{\boldsymbol{p}} \boldsymbol{v}_{\boldsymbol{p}}) \overset{\mathrm{r}}{\rightharpoonup}^{p_n + p'_n} \overset{\mathrm{l}}{\rightharpoonup}^{3q_n} \cdots \overset{\mathrm{r}}{\rightharpoonup}^{p_1 + p'_1} \overset{\mathrm{l}}{\rightharpoonup}^{3q_1} \Phi_{\boldsymbol{p}}(\mathfrak{b}, \boldsymbol{v}_{\boldsymbol{p}}),$$
$$(\mathfrak{b}, \lambda_{\boldsymbol{t}} \boldsymbol{v}_{\boldsymbol{t}}) \overset{\mathrm{r}}{\rightharpoonup}^{t_m + t'_m} \overset{\mathrm{l}}{\rightharpoonup}^{3u_m} \cdots \overset{\mathrm{r}}{\rightharpoonup}^{t_1 + t'_1} \overset{\mathrm{l}}{\rightharpoonup}^{3u_1} \Phi_{\boldsymbol{t}}(\mathfrak{b}, \boldsymbol{v}_{\boldsymbol{t}})$$

form Agol cycles of $\Phi_{\boldsymbol{p}}$ and $\Phi_{\boldsymbol{t}}$ respectively. This together with Remark 2.7 implies that the cyclically ordered sets $\{(p_n + p'_n, 3q_n), \dots, (p_1 + p'_1, 3q_1)\}$ and $\{(t_m + t'_m, 3u_m), \dots, (t_1 + t'_1, 3u_1)\}$ have to be equal. In particular, $n = m$. Up to the shift T, we may assume that

$(*)$ $\boldsymbol{p}, \boldsymbol{t} \in \mathcal{I}_n$ satisfy $p_i + p'_i = t_i + t'_i$ and $q_i = u_i$ for $i = 1, \dots, n$.

The following three cases can occur.

Case 1. $p_i = t_i$ (and $p'_i = t'_i$) for $i = 1, \dots, n$.
Case 2. $p_i = t'_i$ (and $p'_i = t_i$) for $i = 1, \dots, n$.
Case 3. Otherwise,.

In case 1 (resp. case 2) we have $\boldsymbol{p} = \boldsymbol{t}$ (resp. $\boldsymbol{p} = f(\boldsymbol{t})$). In both cases it holds $\boldsymbol{p} \sim \boldsymbol{t}$. We will later show that case 3 cannot occur.

Claim 1. Let $(\mathfrak{b}, \boldsymbol{x})$ be a measured train track in $\Sigma_{1,2}$ as in Figure 2(3). Let $h : \Sigma_{1,2} \to \Sigma_{1,2}$ be an orientation-preserving diffeomorphism preserving the train track $\mathfrak{b}$. Then $h(\mathfrak{b}, \boldsymbol{x}) = (\mathfrak{b}, \boldsymbol{x})$ or $h(\mathfrak{b}, \boldsymbol{x}) = (\mathfrak{b}, J\boldsymbol{x})$, where J is the matrix as in Lemma 4.5.

Proof of Claim 1. Let $\iota : \Sigma_{1,2} \to \Sigma_{1,2}$ be the hyperelliptic involution, exchanging the two punctures. Let $F : \Sigma_{1,2} \to \Sigma_{1,2}$ be the π-rotation as above. Then $\iota(\mathfrak{b}, \boldsymbol{x}) = (\mathfrak{b}, \boldsymbol{x})$, $F(\mathfrak{b}, \boldsymbol{x}) = (\mathfrak{b}, J\boldsymbol{x})$ and $F \circ \iota(\mathfrak{b}, \boldsymbol{x}) = (\mathfrak{b}, J\boldsymbol{x})$. Consider any orientation-preserving diffeomorphism $h : \Sigma_{1,2} \to \Sigma_{1,2}$ preserving the train track $\mathfrak{b}$. Since large branches are mapped to large branches under h, we observe that h is either the identity map 1, ι, F or $F \circ \iota = \iota \circ F$. This completes the proof.

We turn to case 3. For $\boldsymbol{p} \in \mathcal{I}_n$ let $\boldsymbol{v_p}$ be the normalized eigenvector of $M_{\boldsymbol{p}}$ given in Theorem 2.13. If case 3 occurs, we have $s_{\boldsymbol{p}} + s_{\boldsymbol{t}} \neq 1$ by Corollary 2.16(2) and $s_{\boldsymbol{p}} \neq s_{\boldsymbol{t}}$ by Corollary 2.16(3). In particular, $\boldsymbol{v_p} \neq J\boldsymbol{v_t}$ and $\boldsymbol{v_p} \neq \boldsymbol{v_t}$. But since by Claim 1, the only possible diffeomorphisms are 1, ι, F or $F \circ \iota = \iota \circ F$, a diffeomorphism $h : \Sigma_{1,2} \to \Sigma_{1,2}$ with $h(\mathfrak{b}, \boldsymbol{v_p}) = (\mathfrak{b}, c\boldsymbol{v_t})$ for some constant $c > 0$ cannot exist. The periodic splitting sequences of $\Phi_{\boldsymbol{p}}$ and $\Phi_{\boldsymbol{t}}$ are not combinatorially isomorphic because they do not satisfy the condition (2) in Definition 2.4. Therefore, $\Phi_{\boldsymbol{p}}$ and $\Phi_{\boldsymbol{t}}$ are not conjugate to each other by Theorem 2.5. This contradicts the assumption that $\Phi_{\boldsymbol{p}}$ and $\Phi_{\boldsymbol{t}}$ are conjugate. Thus case 3 does not occur and the condition (2) implies the condition (1).

To see that (3) implies (1), suppose that $\phi_{\boldsymbol{p}}$ and $\phi_{\boldsymbol{t}}$ are conjugate in $\mathrm{MCG}(\Sigma_{0,5})$. For the 2-fold branched cover $\Sigma_{1,2} \to \Sigma_{0,5}$ their lifts $\Phi_{\boldsymbol{p}}$ and $\Phi_{\boldsymbol{t}}$ are conjugate in $\mathrm{MCG}(\Sigma_{1,2})$. Then $\boldsymbol{p} \sim \boldsymbol{t}$ by the above argument. This completes the proof. $\square$

Acknowledgement

The first author would like to thank the organizers of the FrontierLab program at Osaka University. The program made it possible for the author to conduct research in Japan. Without it, the paper could not have been written. The second author's research was supported by JSPS KAKENHI Grant Numbers JP21K03247, JP22H01125, JP23H0101.

References

[1] Ian Agol, *Ideal triangulations of pseudo-Anosov mapping tori*, Topology and geometry in dimension three, Contemp. Math., vol. 560, Amer. Math. Soc., Providence, RI, 2011, arXiv:1008.1606, doi:10.1090/conm/560/11087, pp. 1–17.

[2] Ian Agol and Chi Cheuk Tsang, *Dynamics of veering triangulations: infinitesimal components of their flow graphs and applications*, Algebraic and Geometric Topology, to appear, arXiv:2201.02706.

[3] M. Bestvina and M. Handel, *Train-tracks for surface homeomorphisms*, Topology **34** (1995), no. 1, 109–140, doi:110.1016/0040-9383(94)E0009-9.

[4] F. R. Gantmacher, *The theory of matrices. Vols. 2*, Chelsea Publishing Co., New York, 1959, doi:110.1007/978-3-642-99234-6.

[5] Craig D. Hodgson, Ahmad Issa, and Henry Segerman, *Non-geometric veering triangulations*, Exp. Math. **25** (2016), no. 1, 17–45, arXiv:1406.6439.

[6] Keiko Kawamuro and Eiko Kin, *Complete description of agol cycles of pseudo-anosov 3-braids*, preprint: arXiv:2312.04486v1.

[7] Ron. Knott, *An introduction to continued fractions*, `https://r-knott.surrey.ac.uk/Fibonacci/cfINTRO.html`.

[8] R. C. Penner and J. L. Harer, *Combinatorics of train tracks*, Annals of Mathematics Studies, vol. 125, Princeton University Press, Princeton, NJ, 1992, doi:10.1515/9781400882458.

[9] Robert C. Penner, *A construction of pseudo-Anosov homeomorphisms*, Trans. Amer. Math. Soc. **310** (1988), no. 1, 179–197, doi:10.1090/S0002-9947-1988-0930079-9.

Department of Mathematics, Ludwig-Maximilians-University Munich, 80333 Munich, Theresienstr. 39, Germany

Email address: `j.bellynck@campus.lmu.de`

Center for Education in Liberal Arts and Sciences, Osaka University, Toyonaka, Osaka 560-0043, Japan

Email address: `kin.eiko.celas@osaka-u.ac.jp`